HAL
open science

Analysis of explicit and implicit discrete-time equivalent-control based sliding mode controllers

Olivier Huber, Vincent Acary, Bernard Brogliato

To cite this version:

Olivier Huber, Vincent Acary, Bernard Brogliato. Analysis of explicit and implicit discrete-time equivalent-control based sliding mode controllers. [Research Report] RR-8383, INRIA. 2013, pp.23. hal-00875209

HAL Id: hal-00875209

https://inria.hal.science/hal-00875209

Submitted on 21 Oct 2013

HAL is a multi-disciplinary open access archive for the deposit and dissemination of scientific research documents, whether they are published or not. The documents may come from teaching and research institutions in France or abroad, or from public or private research centers.

L'archive ouverte pluridisciplinaire **HAL**, est destinée au dépôt et à la diffusion de documents scientifiques de niveau recherche, publiés ou non, émanant des établissements d'enseignement et de recherche français ou étrangers, des laboratoires publics ou privés.

Analysis of explicit and implicit discrete-time equivalent-control based sliding mode controllers

Olivier Huber, Vincent Acary, Bernard Brogliato

RESEARCH REPORT
N° 8383
October 2013
Project-Team BiPoP

ISSN 0249-6399 ISRN INRIA/RR--8383--FR+ENG

Analysis of explicit and implicit discrete-time equivalent-control based sliding mode controllers

Olivier Huber, Vincent Acary, Bernard Brogliato

Project-Team BiPoP

Research Report n° 8383 — October 2013 — 23 pages

Abstract: Different time-discretization methods for equivalent-control based sliding mode control (ECB-SMC) are presented. A new discrete-time sliding mode control scheme is proposed for linear time-invariant (LTI) systems. It is error-free in the discretization of the equivalent part of the control input. Results from simulations using the various discretized SMC schemes are shown, with and without perturbations. They illustrate the different behaviours that can be observed. Stability results for the proposed scheme are derived.

Key-words: sliding mode control, sampled-data system, discrete-time Lyapunov stability,implicit discretization

RESEARCH CENTRE GRENOBLE – RHÔNE-ALPES

Inovallée
655 avenue de l'Europe Montbonnot
38334 Saint Ismier Cedex

Analyse de la discretization explicite ou implicite des controlleurs par modes glissants

Résumé : Dans ce rapport, differentes techniques de discretisation temporelle pour le contrôle par modes glissants sont présentées. Une nouvelle structure de contrôle par modes glissants est proposée pour des systèmes linéaires invariants. Elle ne comporte pas d'erreur dans la discretisation de la partie équivalente du contrôle. Des résultats de simulations avec divers contrôlleurs par modes glissants sont présentées, avec ou sans perturbation. Ils illustrent les phénomènes qui peuvent être observés suivant le type de discretisation utilisé. Pour finir, la stabilité de la nouvelle structure de contrôle est étudiée.

Mots-clés : contrôle par modes glissants, système échantionnés, stabilité de Lyapunov en temps discret, discretisation implicite

1 Introduction

The time discretization of sliding-mode controllers has witnessed an intense activity in the past 30 years [1–6] and [7]. This concerns in particular the classical Equivalent-Control-Based Sliding-Mode Control (ECB-SMC), which consists of two sub-controllers: the state-continuous equivalent control u^{eq} and the state-discontinuous control u^s. In these past research efforts, most of the focus was on the discontinuous part of the control, since it introduces numerical chattering. Several solutions to alleviate numerical chattering (that is solely due to the time discretization [8–12]) have been proposed [1–7,13,14], most of them consisting in the definition of a so-called quasi-sliding surface [5] and an explicit discretization of u^s. The works in [2] and [6] depart from these discrete-time controllers and propose an algorithm which allows the sliding variable to take exactly the zero value at sampling times. They are however limited to first order, scalar systems and require some stringent assumptions. Recently a new approach, which may be seen as a (non-trivial) extension of the controllers in [2] and [6], has been proposed in [11] and [12]. The basic idea is to implement the discontinuous input u^s in an implicit form, while keeping its causality (i.e. the controller is nonanticipative). Then this input has to be computed at each sampling time as the solution to a generalized, set-valued equation, which takes the form of a simple projection on an interval in the simplest cases. Let us illustrate the difference between explicit and implicit discretization with an academic example, $\dot{x}(t) \in -\alpha \operatorname{sgn}(x(t))$, $\alpha > 0$. We use the differential inclusion framework since we let $\operatorname{sgn}(0)$ to take any value in $[-1, 1]$ (this is formally stated in Definition 1 as Sgn). An explicit discretization yields $x(t_{k+1}) \in x(t_k) - h\alpha \operatorname{sgn}(x(t_k))$, whereas the implicit one yields $x(t_{k+1}) \in x(t_k) - h\alpha \operatorname{sgn}(x(t_{k+1}))$. As long as $|x(t_k)| \gg h\alpha$, there is no difference between the two discretizations. But if $|x(t_k)| < \alpha h$, then the behaviour changes with the type of discretization. With $0 < x(t_k) < h\alpha$, in the explicit case, $x(t_{k+1}) \in x(t_k) - h\alpha \operatorname{sgn}(x(t_k)) < 0$. The sign of the state will change at every t_k, leading to the well-known chattering phenomenon. Whereas in the implicit case, it is possible to ensure $x(t_{k+1}) = 0$ by choosing $\operatorname{sgn}(x(t_{k+1})) = x(t_k)/(\alpha h) < 1$. The implicit discretization of the sign function is rigorously presented in Section 3.

To the best of our knowledge, the discretization of the equivalent part has received little attention. In this work, we present a study of the effects of discretization on both the equivalent and discontinuous part of the control. After studying the different discretization methods and their shortcomings, we propose a new discrete-time control scheme, where the equivalent part is not a discretized version of its continuous-time counterpart but is directly designed from the discrete-time dynamics. Some properties of this scheme, like finite-time convergence to the sliding surface and perturbation attenuation, are studied in Section 7.

In this paper, we consider systems of the form

$$\begin{cases} \dot{x}(t) = Ax(t) + Bu(t) + B\xi(t) \\ u(t) = u^{eq}(t) + u^s(t) \\ \sigma(t) := Cx(t) \\ u^s(t) \in -\alpha \operatorname{Sgn}\left(\sigma(x(t))\right), \end{cases} \tag{1}$$

with $x(t) \in \mathbb{R}^n, u(t) \in \mathbb{R}^p, \sigma(t) \in \mathbb{R}^p$, $C \in \mathbb{R}^{p\times n}$, and $\alpha > 0$. The function σ is called the *sliding variable*, the disturbance is denoted as ξ, and Sgn is formally introduced in Definition 1. The perturbation ξ is supposed to be at least continuous: noise is not considered in this paper. When $\xi = 0$, the system is said to be *nominal*. The method used to discretize the dynamics is called Zero-Order Hold (ZOH), also known as exact sampled-data representation. It is often considered for technological reasons, but also because there is no error with this discretization method.

In the remainder of this section, we introduce the notation. In Section 2 we briefly recall the ECB-SMC theory. Then some classical discretization methods are presented in Section 3. Section 4 is dedicated to the discrete error analysis of various controllers of Section 3. We introduce our new discrete-time SMC scheme in Section 5. Simulation results using different time-discretization methods are shown in Section 6, to illustrate the possible different behaviours of the closed-loop system. Finally, stability results are derived in Section 7. Conclusions end the paper in Section 8.

Notations: Let $\mathbf{x}\colon \mathbb{R}_+ \times \mathbb{R}^p \times \mathbb{R}^n \to \mathbb{R}^n$ be the solution of system (1), $x := \mathbf{x}(\,\cdot\,, u, x_0)$ is the solution associated with a continuous-time control u and an initial state $x_0 \in \mathbb{R}^n$, while $\bar{x} := \mathbf{x}(\,\cdot\,, \bar{u}, x_0)$ is the solution with a step function $\bar{u}$ and the same initial state. In the latter case, we denote by $\bar{\sigma} := C\bar{x}$ the sliding variable. The control values change at predefined time instants t_k, defined for all $k \in \mathbb{N}:\ t_k := t_0 + kh,\ t_0, h \in \mathbb{R}_+$. The scalar h is called the timestep. We denote $\bar{x}_k := \bar{x}(t_k)$ and $\bar{\sigma}_k := \bar{\sigma}(t_k)$ for all $k \in \mathbb{N}$. For all $y \in \mathbb{R}^r$, $\|y\|_\infty = \max_i |y_i|$. For all $M \in \mathbb{R}^{r\times s}$, $\|M\|_\infty = \max_i \sum_j |M_{ij}|$. Let $w\colon \mathbb{R} \to \mathbb{R}^r$ and S be any interval in $\mathbb{R}$, $\|w\|_{\infty,S} = \max_i \operatorname{ess\,sup}_{t\in S} |w_i(t)|$. Let $\langle\,\cdot\,,\,\cdot\,\rangle$ denote the standard inner product in a Euclidean space and $\|\cdot\|$ the norm based upon it. Let sgn be the classical single-valued sign function: for all $x > 0$, $\operatorname{sgn}(x) = 1$, $\operatorname{sgn}(-x) = -1$ and $\operatorname{sgn}(0) = 0$.

Definition 1 (Multivalued sign function)**.** Let $x \in \mathbb{R}$. The multivalued sign function $\mathrm{Sgn}\colon \mathbb{R} \rightrightarrows \mathbb{R}$ is defined as:

$$\mathrm{Sgn}(x) = \begin{cases} 1 & x > 0 \\ -1 & x < 0 \\ [-1, 1] & x = 0. \end{cases} \tag{2}$$

If $x \in \mathbb{R}^n$, then the multivalued sign function $\mathrm{Sgn}\colon \mathbb{R}^n \rightrightarrows \mathbb{R}^n$ is defined as: for all $j = 1, \dots, n$, $(\mathrm{Sgn}(x))_j \coloneqq \mathrm{Sgn}(x_j)$.

Definition 2. Let $f\colon \mathbb{R}^n \times \mathbb{R} \to \mathbb{R}^p$ and $l \in \mathbb{R}$. One has $f = \mathcal{O}(h^l)$ if for all $x \in \mathbb{R}^n$, there exists $c \in \mathbb{R}^p$ such that $f(x, h)/h^l \to c$ as $h \to 0$.

Definition 3. [15, p. 147] Let $M \in \mathbb{R}^{n\times n}$. M is a **P**-matrix if for all $x \in \mathbb{R}^n$ such that for all $i \in \{1, \dots, n\}$, $x_i(Mx)_i \leq 0$, then $x = 0$.

Lemma 1. *[15, p. 147] Let $M \in \mathbb{R}^{n\times n}$. If M is positive-definite, then M is a* **P***-matrix.*

2 The equivalent-based continuous-time sliding-mode controller

Let us assume that the triplet (A, B, C) has a strict vector relative degree $(1, 1, \dots, 1)$. This implies that the decoupling matrix CB is full rank. The dynamics of the sliding variable in the nominal system (1) (that is with $\xi(t) = 0$) is

$$\dot{\sigma}(t) = CAx(t) + CBu^{eq}(t) + CBu^s(t). \tag{3}$$

The control law u^{eq} is designed such that the system stays on the sliding surface once it has been reached (in other word u^{eq} renders the sliding surface invariant with $u^s \equiv 0$):

$$\dot{\sigma}(t) = 0 \text{ and } u^s(t) = 0 \quad \Rightarrow \quad u^{eq}(t) = -(CB)^{-1}CAx(t). \tag{4}$$

Then the sliding variable dynamics with the equivalent control reduces to

$$\begin{cases} \dot{\sigma}(t) = CBu^s(t) \\ u^s(t) \in -\alpha\,\mathrm{Sgn}(\sigma(t)). \end{cases} \tag{5}$$

The nominal system (1) can be rewritten as

$$\dot{x}(t) = (I - B(CB)^{-1}C)Ax(t) + Bu^s(t), \tag{6}$$

or equivalently

$$\dot{x}(t) = \Pi Ax(t) + Bu^s(t), \tag{7}$$

with $\Pi \coloneqq I - B(CB)^{-1}C$. Two interesting properties of Π are $C\Pi = 0$ and Π is a projector [16]. Taking the integral form of system (7) yields the relation

$$x(t) = \Phi(t, t_0)x(t_0) + \int_{t_0}^{t} \Phi(t, \tau)Bu^s(\tau)\mathrm{d}\tau, \tag{8}$$

with $\Phi(t, t_0) = e^{\Pi A(t-t_0)}$ the state transition matrix for the system (7). Some of the properties of Φ are given in the following lemma.

Lemma 2. *One has $\dot{\Phi}(t, t_0) = \Pi A\Phi(t, t_0)$, $\Phi(t_0, t_0) = I$, and $C\Phi = C$ for all $t \geq t_0$.*

Proof. One has $C\dot{\Phi}(t, t_0) = 0$ so $C\Phi(t, t_0) = C\Phi(t_0, t_0) = C$ for all $t \geq t_0$. □

3 Discrete-time controllers

3.1 Classical discretization methods to obtain discrete-time controllers

From now on, $\bar{u}^{eq}$ and $\bar{u}^s$ are sampled control laws defined as right-continuous step functions:

$$\bar{u}^{eq}(t) = \bar{u}_k^{eq}, \quad t \in [t_k, t_{k+1}) \tag{9}$$

$$\bar{u}^s(t) = \bar{u}_k^s, \quad t \in [t_k, t_{k+1}). \tag{10}$$

The goal of the discretization process is to choose the elements of the sequences $\{\bar{u}_k^{eq}\}$ and $\{\bar{u}_k^s\}$ such that the discrete-time system exhibits properties as close as possible to the ones with a continuous-time controller. In continuous time, sliding-mode controlled systems have their evolution divided into two phases: the *reaching phase*, where $\|\sigma\| > 0$ and is decreasing, and the *sliding phase*, where $\sigma = 0$ and the sliding motion occurs. It is well known that the sliding motion does not occur in general in discrete time even on a nominal system because of the error induced by the discretization. This has led to the definition of quasi-sliding surfaces [5]. By analogy with the Filippov's solutions we define the following.

Definition 4 (Discrete-time sliding phase)**.** A system (1), in its sampled-data form, is in the discrete-time sliding phase if $\bar{u}^s$ takes values in $(-\alpha, \alpha)^p$.

Such a definition appears to be new in the discrete-time sliding mode control field since it implies that the discrete-time discontinuous controller is itself set-valued, just as its continuous-time counterpart in (1) and (5). This will be made possible with an implicit implementation, as proved in [11] and [12]. It is crucial not to define the sliding phase in terms of $\bar{\sigma}_k$, but rather in terms of the discontinuous input $\bar{u}^s$. In continuous-time, Definition 4 applied to u^s implies that the system is in the sliding phase $\sigma \equiv 0$, see (5). It holds with a matched perturbation as long as for all $t \geq 0$, $\|\xi(t)\|_\infty \leq \delta < \alpha$ for some $\delta \geq 0$.

Integrating the nominal version of (1) over $[t_k, t_{k+1})$ and using the expressions in (10), we obtain the ZOH discretization of the system:

$$\bar{x}_{k+1} = e^{Ah}\bar{x}_k + B^*\bar{u}_k^{eq} + B^*\bar{u}_k^s, \tag{11}$$

with

$$B^* := \int_{t_k}^{t_{k+1}} e^{A(t_{k+1}-\tau)} B \mathrm{d}\tau. \tag{12}$$

Let $\Psi := \int_{t_k}^{t_{k+1}} e^{A(t_{k+1}-\tau)}\mathrm{d}\tau = \sum_{l=0}^{\infty} \frac{A^l h^{l+1}}{(l+1)!}$, then $B^* = \Psi B$. We now present different choices for the values $\bar{u}_k^{eq}$ and $\bar{u}_k^s$. Firstly, standard methods are described, while the new method is studied in the next section. Here $\bar{u}_k^{eq}$ and $\bar{u}_k^s$ are the discretized values of the continuous-time control law u^{eq} and u^s. From all the possible time-discretization schemes, we focus on the one-step explicit, implicit, and midpoint ones. With the expressions found for u^{eq} and u^s in (4) and (5), the proposed discretized values for the equivalent control $\bar{u}_k^{eq}$ are:

$$\bar{u}_{k,e}^{eq} = -(CB)^{-1}CA\bar{x}_k \qquad \text{explicit input,} \tag{13a}$$

$$\bar{u}_{k,i}^{eq} = -(CB)^{-1}CA\bar{x}_{k+1} \qquad \text{implicit input,} \tag{13b}$$

$$\bar{u}_{k,m}^{eq} = 1/2(\bar{u}_{k,e}^{eq} + \bar{u}_{k,i}^{eq}) \qquad \text{midpoint input,} \tag{13c}$$

and the two possibilities for the discontinuous control $\bar{u}_k^s$ are:

$$\bar{u}_k^s = -\alpha\,\mathrm{sgn}(\bar{\sigma}_k) \qquad \text{explicit input,} \tag{14a}$$

$$\bar{u}_k^s \in -\alpha\,\mathrm{Sgn}(\bar{\sigma}_{k+1}) \qquad \text{implicit input.} \tag{14b}$$

We use the singled-valued sgn function in (14a) since the case $\bar{\sigma}_k = 0$ is not worth considering for explicit inputs. Moreover with the set-valued Sgn function, if $\bar{\sigma}_k = 0$, then we would have $\mathrm{Sgn}(\bar{\sigma}_k) \in [-\alpha, \alpha]^p$ and there is no proper selection procedure to get a value for $\bar{u}_k^s$. In the next subsection, we present the selection procedure in the implicit case. The objective in Section 6 is to study the behaviour of the closed-loop system when different combinations of equations (13a)–(13c) and (14a)–(14b) are used. The most commonly used control law is the combination of (13a) and (14a). This kind of discretization has been studied in [8, 9, 17], with a focus on the sequence formed by $\bar{\sigma}_k$ once the system state approaches the sliding manifold. The implicit discretization (14b) was first introduced in [11] and [12]. In the following, we provide more details on it.

3.2 Definition and properties of the implicitly discretized discontinuous control input

With the implicit method (14b), for each $k \in \mathbb{N}$, $\bar{u}_k^s$ is computed as the solution to the generalized equation

$$\begin{cases} \widetilde{\sigma}_{k+1} = \bar{\sigma}_k + CB^* \bar{u}_k^s \\ \bar{u}_k^s \in -\alpha \operatorname{Sgn}(\widetilde{\sigma}_{k+1}). \end{cases} \tag{15}$$

As shown in [11], there exists $k_0 \in \mathbb{N}$ such that for all $k > k_0$, $\widetilde{\sigma}_k = 0$. Let us write the discrete-time system with an implicit discretization of u^s and let $\bar{u}_k^{eq}$ be computed using one of the methods in equations (13a)–(13c):

$$\begin{cases} \bar{x}_{k+1} = e^{Ah}\bar{x}_k + B^*\bar{u}_k^{eq} + B^*\bar{u}_k^s \\ \widetilde{\sigma}_{k+1} = C\bar{x}_k + CB^*\bar{u}_k^s \\ \bar{u}_k^s \in -\alpha \operatorname{Sgn}(\widetilde{\sigma}_{k+1}). \end{cases} \tag{16}$$

Nothing guarantees that $C(e^{Ah}\bar{x}_k + B^*\bar{u}_k^{eq}) = C\bar{x}_k$. Hence, $\widetilde{\sigma}_{k+1}$ is in general different from $\bar{\sigma}_{k+1}$ because of the discretization error on u^{eq}. Indeed this error, stemming from the discretization of u^{eq}, can be seen as a perturbation of the closed-loop system, even if $\xi \equiv 0$. Therefore, $\widetilde{\sigma}_{k+1}$ can be considered as an approximation of $\bar{\sigma}_{k+1}$.

The system (15) can be analysed using the Affine Variational Inequality (AVI) formalism [18]. Let $N_{[-\alpha,\alpha]^p}(\lambda)$ be the normal cone to the box $[-\alpha,\alpha]^p$ at λ, that is $N_{[-\alpha,\alpha]^p}(\lambda) = \{d \in \mathbb{R}^p \mid \langle d, y-\lambda\rangle \leq 0, \forall y \in [-\alpha,\alpha]^p\}$. The relation $\bar{u}_k^s \in -\operatorname{Sgn}(\widetilde{\sigma}_{k+1}) \iff \widetilde{\sigma}_{k+1} \in -N_{[-\alpha,\alpha]^p}(\bar{u}_k^s)$ enables us to transform (15) into the inclusion:

$$0 \in \bar{\sigma}_k + CB^*\bar{u}_k^s + N_{[-\alpha,\alpha]^p}(\bar{u}_k^s). \tag{17}$$

The inclusion (17) is satisfied if and only if $\bar{u}_k^s$ is the solution of the AVI:

$$\text{Find } z \in [-\alpha,\alpha]^p \text{ such that} \quad (y-z)^T(\bar{\sigma}_k + CB^*z) \geq 0, \quad \forall y \in [-\alpha,\alpha]^p. \tag{18}$$

Let $\mathrm{SOL}(CB^*, C\bar{x}_k)$ denote the set of all solutions to the AVI (18). The existence and uniqueness of solutions to this AVI are now presented.

Lemma 3. *The AVI* (18) *has always a solution.*

Proof. Since the mapping $z \mapsto CB^*z + \bar{\sigma}_k$ is continuous, we can apply the Corollary 2.2.5, p. 148 in [18]. □

Lemma 4. *The AVI* (18) *has a unique solution for all* $\bar{\sigma}_k \in \mathbb{R}^n$ *if and only if* CB^* *is a* **P***-matrix.*

Proof. In [18], using Theorem 4.3.2 p. 372 and Example 4.2.9 p. 361 yields the result. □

In most ECB-SMC systems, $CB^* > 0$, therefore is a **P**-matrix. This approach enables us to analyse a large class of systems, compared to previous approaches where it is supposed that CB^* is scalar [6]. The solution is a function of $\bar{\sigma}_k$ (hence $\bar{x}_k$) and if CB^* is a **P**-matrix, the solution map $C\bar{x}_k \mapsto \bar{u}_k^s = \mathrm{SOL}(CB^*, \bar{\sigma}_k)$ is Lipschitz continuous. When the control is scalar or if CB^* is diagonal, a solution to (15) can be computed as a simple orthogonal projection: $\bar{u}_k^s = -\operatorname{proj}_{[-\alpha,\alpha]^p}((CB^*)^{-1}\bar{\sigma}_k)$. Otherwise a quadratic problem with bounded constraints may be considered [12]. More details on the numerical aspects and solvers for this kind of problems can be found in [15] and [19]. Now that we have discussed the existence, uniqueness, some properties of solutions and methods to compute them, we turn our attention to the performance of each controller.

4 Discretization performance

4.1 Discretization of the state-continuous control

Let us focus on the discretization error on u^{eq} and more specifically on its effect on the sliding variable. In other words we analyse how the invariance property in (4) is preserved after discretization. In the following, $\bar{u}^s$ is set to 0. Let $\Delta\bar{\sigma}_k := \bar{\sigma}_{k+1} - \bar{\sigma}_k$ be the local variation of the sliding variable due to the discretization error on u^{eq}.

4.1.1 Explicit discretization

With an explicit discretization of u^{eq} as in (13a), and using (11) the closed-loop discrete-time system dynamics is

$$\bar{x}_{k+1} = \Phi_k^e \bar{x}_k, \tag{19}$$

with $\Phi_k^e := e^{Ah} - \Psi\Pi_B A$ and $\Pi_B := B(CB)^{-1}C = I - \Pi$.

Lemma 5. *With an explicit discretization of u^{eq}, the discretization error $\Delta\bar{\sigma}_k$ is of order $\mathcal{O}(h^2)$.*

Proof. Starting from (19), one obtains

$$\bar{x}_{k+1} - \bar{x}_k = (e^{Ah} - I)\bar{x}_k - \Psi\Pi_B A\bar{x}_k. \tag{20}$$

Hence, using the definition of Ψ in Section 3.1:

$$\begin{aligned}
\Delta\bar{\sigma}_k = \bar{\sigma}_{k+1} - \bar{\sigma}_k &= C\left(e^{Ah} - I - \Psi\Pi_B A\right)\bar{x}_k && (21)\\
&= C\left(Ah + \frac{A^2h^2}{2} - \left(h + \frac{Ah^2}{2}\right)\Pi_B A + \mathcal{O}(h^3)\right)\bar{x}_k && (22)\\
&= C\left(\left(h + \frac{Ah^2}{2}\right)(I - \Pi_B)A\right)\bar{x}_k + \mathcal{O}(h^3) && (23)\\
&= hC\Pi A\bar{x}_k + \frac{h^2}{2}CA\Pi A\bar{x}_k + \mathcal{O}(h^3) && (24)\\
&= \frac{h^2}{2}CA\Pi A\bar{x}_k + \mathcal{O}(h^3). && (25)
\end{aligned}$$

The action of $u_{k,e}^{eq}$ does not keep $\bar{\sigma}$ constant and the error is of order $\mathcal{O}(h^2)$. □

4.1.2 Implicit discretization

The recurrence equation (11) combined with (13b) yields

$$\bar{x}_{k+1} = e^{Ah}\bar{x}_k - \Psi\Pi_B A\bar{x}_{k+1}, \tag{26}$$

that is:

$$\bar{x}_{k+1} = W^{-1}e^{Ah}\bar{x}_k, \tag{27}$$

with $W = I + \Psi\Pi_B A$.

Lemma 6. *With an implicit discretization of u^{eq}, the discretization error $\Delta\bar{\sigma}_k$ is of order $\mathcal{O}(h^2)$.*

Proof. There exists a Taylor expansion for W^{-1} if $\Psi\Pi_B A$ has all its eigenvalues in the unit disk. Since $\Psi \to 0$ as $h \to 0$, it is always possible to find an h_0 such that this condition holds for all $h_0 > h > 0$. Since we are interested in an asymptotic property, such restriction on h does not play any role. Let us compute the finite expansion of $W^{-1}e^{Ah}$:

$$\begin{aligned}
W^{-1}e^{Ah} &= \left(I - \Psi\Pi_B A + (\Psi\Pi_B A)^2\right)\left(I + Ah + \frac{A^2h^2}{2}\right) + \mathcal{O}(h^3) && (28)\\
&= I - \Psi\Pi_B A + Ah + (\Psi\Pi_B A)^2 - h\Psi\Pi_B A^2 + \frac{A^2h^2}{2} + \mathcal{O}(h^3) && (29)\\
&= I - (\Pi_B A - A)h + \left(-\frac{\Pi_B A\Pi_B A}{2} + \Pi_B A\Pi_B A - \Pi_B A^2 + \frac{A^2}{2}\right)h^2 + \mathcal{O}(h^3) && (30)\\
&= I - (\Pi_B A - A)h + \left(\frac{\Pi_B A\Pi_B A}{2} - \Pi_B A^2 + \frac{A^2}{2}\right)h^2 + \mathcal{O}(h^3). && (31)
\end{aligned}$$

Then the variation of the sliding variable is

$$\Delta\bar{\sigma}_k = C(W^{-1}e^{Ah} - I)\bar{x}_k = h(-A + A)\bar{x}_k + h^2\left(\frac{CA\Pi_B A}{2} - \frac{CA^2}{2}\right)\bar{x}_k + \mathcal{O}(h^3) \tag{32}$$

$$= \frac{h^2}{2} CA(I - \Pi_B)A\bar{x}_k + \mathcal{O}(h^3) \tag{33}$$

$$= -\frac{h^2}{2} CA\Pi A\bar{x}_k + \mathcal{O}(h^3). \tag{34}$$

□

Lemma 7. *With a midpoint method* (13c)*, the error is of order* $\mathcal{O}(h^3)$*.*

Proof. With the midpoint method (13c), the recurrence equation is

$$\bar{x}_{k+1} = 1/2(e^{Ah}\bar{x}_k - \Psi\Pi_B A\bar{x}_k) + 1/2(e^{Ah}\bar{x}_k - \Psi\Pi_B A\bar{x}_{k+1}). \tag{35}$$

The two terms are the right-hand side in (20) and (26). Then the discretization error is the mean of the discretization error of the explicit and implicit case. Since the first term in (34) is the opposite of the first one in (25), the term in h^2 vanishes and the error is of order $\mathcal{O}(h^3)$. □

4.2 Discretization of both control inputs

In the following, we consider the sliding variable dynamics with the state-continuous and discontinuous control. It is expected that $\bar{\sigma}$ goes to 0 and once it reaches zero, stays at this value. The proposed metric to measure the performance of the discrete-time controller is the Euclidean norm of the sliding variable when the system state is close to the sliding manifold. Let $\varepsilon_k := \|\bar{\sigma}_{k+1}\|$ be the discretization error when $\|\bar{\sigma}_k\|$ is small enough.

4.2.1 Explicit discretization

In the sliding mode literature, several proposals (seven of them are listed in [20]) have been made to analyse the behaviour of the closed-loop system near the sliding manifold and to propose new variable structure control strategies. Despite this, it is still difficult to analyse the behaviour near the sliding manifold, besides stability. Thus we only study the invariance of a close neighborhood of the sliding manifold, also to provide an estimate of the chattering due to the discrete discontinuous control.

Lemma 8. *Let the closed-loop system state in* (11) *be in an* $\mathcal{O}(h^2)$*-neighborhood of the sliding manifold at* $t = t_k$*, i.e.* $\bar{\sigma}_k = \mathcal{O}(h^2)$*, but with* $\bar{\sigma}_k \neq 0$*. If the discontinuous part* u^s *of the control is discretized using the explicit scheme* (14a)*, then the discretization error* ε_k *is of order* $\mathcal{O}(h)$ *and the system exits the* $\mathcal{O}(h^2)$*-neighborhood.*

Proof. Starting from equation (11) and using the control inputs $\bar{u}_k^{eq} = -(CB^*)^{-1}CA\bar{x}_k$ and $\bar{u}_k^s = -\alpha\,\mathrm{sgn}(C\bar{x}_k)$, we have the following:

$$\bar{\sigma}_{k+1} = C(e^{Ah} - \Psi\Pi_B A)\bar{x}_k - CB^*\,\mathrm{sgn}(C\bar{x}_k) \tag{36}$$

that is

$$\bar{\sigma}_{k+1} = \bar{\sigma}_k + \Delta_k - CB^*\,\mathrm{sgn}(\bar{\sigma}_k), \tag{37}$$

with

$$\Delta_k := C(e^{Ah} - I - \Psi\Pi_B A)\bar{x}_k. \tag{38}$$

Let us study the square of the norm of the sliding variable:

$$\bar{\sigma}_{k+1}^T\bar{\sigma}_{k+1} = \|\bar{\sigma}_k\|^2 + \|\Delta_k\|^2 + \|CB^*\,\mathrm{sgn}(\bar{\sigma}_k)\|^2 + \bar{\sigma}_k^T\Delta_k - \bar{\sigma}_k^T CB^*\,\mathrm{sgn}(\bar{\sigma}_k) - \Delta_k^T CB^*\,\mathrm{sgn}(\bar{\sigma}_k). \tag{39}$$

From Lemma 5, we have $\|\Delta_k\|^2 = \mathcal{O}(h^4)$. For each other term, we can compute its order with respect to h:

$$\|CB^*\alpha\,\mathrm{sgn}(\bar{\sigma}_k)\|^2 = \left\|\sum_{k=0}^{\infty} h^{l+1}\frac{CA^lB}{(l+1)!}\alpha\,\mathrm{sgn}(\bar{\sigma}_k)\right\|^2$$

$$\leq \|hCB\alpha\,\mathrm{sgn}(\bar{\sigma}_k)\|^2 + \mathcal{O}(h^3) \tag{40}$$

$$\Delta_k^T CB^*\alpha\,\mathrm{sgn}(\bar{\sigma}_k) = \mathcal{O}(h^3). \tag{41}$$

Using the Cauchy-Schwarz inequality on the remaining terms yields

$$|\bar{\sigma}_k^T \Delta_k| \leq \|\bar{\sigma}_k\| \|\Delta_k\| \tag{42}$$

$$|\bar{\sigma}_k^T CB^* \operatorname{sgn}(\bar{\sigma}_k)| \leq \|\bar{\sigma}_k\| \|CB^* \operatorname{sgn}(\bar{\sigma}_k)\|. \tag{43}$$

If $\|\bar{\sigma}_k\| = \mathcal{O}(h^2)$, then the above terms are of order $\mathcal{O}(h^4)$ and $\mathcal{O}(h^3)$. Hence, the dominant term in (39) will be $\|hCB\alpha \operatorname{sgn}(\bar{\sigma}_k)\|^2$. Let $\{\lambda_i\}$ be the spectrum of hCB, with $\lambda_m = \min_i |\lambda_i|$ and $\lambda_M = \max_i |\lambda_i|$. We have the following:

$$\lambda_m h\alpha\sqrt{p} \leq \|hCB \operatorname{sgn}(\bar{\sigma}_k)\| \leq \lambda_M h\alpha\sqrt{p}. \tag{44}$$

Inserting this in (39) yields that $\|\bar{\sigma}_{k+1}\|$ has order $\mathcal{O}(h)$. □

Therefore with an explicit discretization of u^s, the main error comes from the discretization of the discontinuous control u^s, since it increases the error by an order h.

4.2.2 Implicit discretization

In the following, we are interested in studying the discretization error in the same context as for the previous lemma.

Lemma 9. *Let the closed-loop system be in the discrete-time sliding phase, as defined in Definition 4. If the discontinuous part u^s of the control is discretized using an implicit scheme, then the discretization error ε_k has the same order as the discretization error $\Delta\bar{\sigma}_k$ on u^{eq}. That is $\mathcal{O}(h^2)$ for the methods* (13a) *and* (13b)*, and $\mathcal{O}(h^3)$ for the midpoint method* (13c)*.*

Proof. Let $\Delta_k = C(e^{Ah} - I)x_k + C\Psi B\bar{u}_k^{eq}$, with $\bar{u}_k^{eq}$ any method in (13a)-(13c). The system is supposed to be in the discrete-time sliding phase, that is $u_k^s \in (-\alpha, \alpha)^p$. Then $\widetilde{\sigma}_{k+1} = \bar{\sigma}_k + CB^*\bar{u}_k^s = 0$. From (11) one has:

$$\bar{\sigma}_{k+1} = \bar{\sigma}_k + \Delta_k + CB^*\bar{u}_k^s = \Delta_k \tag{45}$$

Let us go through all the possible discretization of u^{eq}. In the explicit case (13a), Δ_k is the quantity studied in (21)-(25) and is of order $\mathcal{O}(h^2)$. With the implicit method (13b), the order of Δ_k is $\mathcal{O}(h^2)$, as shown in (32)-(34). With the midpoint method (13c), going along the lines of the proof of Lemma 7, we get that Δ_k is of order $\mathcal{O}(h^3)$. □

Remark 1. In Section 7, conditions are derived to ensure that the system stays in the discrete-time sliding phase once it reaches it, with or without perturbation.

4.3 Disturbance and chattering

We consider the system (1) with a non-zero perturbation. In the following we consider only continuous perturbations. Let us first recall some facts with a continuous-time controller. The design procedure for the equivalent part is the same as in the unperturbed case. If the system is in the sliding phase, it can stay on the sliding surface despite the perturbation $\xi(t)$, if the origin is contained in the set obtained using the Filippov's convexification procedure. We suppose here that CB is nonsingular. Then the condition for rejection can be reformulated as $0 \in -\alpha \operatorname{Sgn}(0) + \xi(t)$. The condition $\alpha > \|\xi\|_\infty$ ensures the unconditional existence of the sliding motion.

We now investigate the performance of the discretization scheme with respect to the perturbation. First we analyse how the perturbation affects the discrete-time dynamics of the system. To take it into account, we just need to add a term $p_k := \int_{t_k}^{t_{k+1}} e^{A(t_{k+1}-\tau)} B\xi(\tau)\mathrm{d}\tau$ to the recurrence relation (11). This yields:

$$\bar{x}_{k+1} = e^{Ah}\bar{x}_k + B^*\bar{u}_k^{eq} + B^*\bar{u}_k^s + p_k. \tag{46}$$

Note that with the type of perturbation we consider, p_k is of order $\mathcal{O}(h^2)$.

4.3.1 Explicit case

Given the expression in (46), to take into account the perturbation, we just have to add the term Cp_k to (37):

$$\bar{\sigma}_{k+1} = \bar{\sigma}_k + \Delta_k - CB^* \operatorname{sgn}(\bar{\sigma}_k) + Cp_k. \tag{47}$$

Using the same analysis as in the previous subsection, that is computing $\|\bar{\sigma}_{k+1}\|^2$, we have all the terms in (39), plus the following:

$$|\bar{\sigma}_k^T Cp_k| \leq \|\bar{\sigma}_k\| \|Cp_k\| = \mathcal{O}(h^3) \quad \text{by Cauchy-Schwarz inequality} \tag{48}$$

$$|\Delta_k^T C p_k| \leq \|\Delta_k\| \|C p_k\| = \mathcal{O}(h^3) \quad \text{by Cauchy-Schwarz inequality} \tag{49}$$

$$(CB^* \alpha \operatorname{sgn}(\bar{\sigma}_k))^T C p_k = \mathcal{O}(h^2) \tag{50}$$

$$\|C p_k\|^2 = \mathcal{O}(h^2). \tag{51}$$

Thus the dominant terms in (47) are of order h and are: $\|Cp_k\|$, $\|CB^*\alpha \operatorname{sgn}(\bar{\sigma}_k)\|$ and $(CB^*\alpha \operatorname{sgn}(\bar{\sigma}_k))^T Cp_k$. Those terms induce chattering and they all have the same order with respect to the timestep h.

4.3.2 Implicit case

Updating (45) to take into account the perturbation yields:

$$\bar{\sigma}_{k+1} = \bar{\sigma}_k + \Delta_k - CB^* \operatorname{sgn}(\bar{\sigma}_{k+1}) + Cp_k \tag{52}$$

$$= \Delta_k + Cp_k. \tag{53}$$

Recall that Δ_k has order $\mathcal{O}(h^2)$. Hence the chattering due to the perturbation will be predominant. In the next Section, we present a method for computing $\bar{u}_k^{eq}$ such that the discretization error $\Delta_k = 0$. Then the chattering is solely due to the perturbation.

5 Exact discrete equivalent control

Let us propose a new control scheme for a discrete-time LTI plant using sliding mode control. Its derivation is along the same lines as in Section 2, that is we first design the equivalent control $\bar{u}^{eq}$ and then the discontinuous part $\bar{u}^s$.

As showed in (5), u^{eq} is defined such that the dynamics of the sliding variable depends only on the input u^s. Starting from (11) and left multiplying by C, one obtains:

$$C\bar{x}_{k+1} = Ce^{Ah}\bar{x}_k + CB^*\bar{u}_k^{eq} + CB^*\bar{u}_k^s. \tag{54}$$

Using (8) with $t = t_{k+1}$ and $t_0 = t_k$, we obtain

$$\sigma(t_{k+1}) = C\Phi(t_{k+1}, t_k)x(t_k) + C\int_{t_k}^{t_{k+1}} \Phi(t_{k+1}, \tau)Bu^s(\tau)\mathrm{d}\tau. \tag{55}$$

Our goal is to have $C\bar{x}_{k+1} = Cx(t_{k+1})$ if $x(t_k) = \bar{x}_k$ and both u^s and $\bar{u}^s$ set to 0. Then setting the last term of (54) and (55) to 0 and using Lemma 2, the following condition holds:

$$C\Phi(t_{k+1}, t_k)x(t_k) = Ce^{Ah}\bar{x}_k + CB^*\bar{u}_k^{eq}, \tag{56}$$

that is

$$CB^*\bar{u}_k^{eq} = C(I - e^{Ah})\bar{x}_k. \tag{57}$$

In [3], this expression for the equivalent control was already derived, when the sliding variable is scalar. In [4], using a deadbeat-like approach, a term similar to (57) can also be found. If we substitute this expression for $\bar{u}_k^{eq}$ in (54), then, as expected, we obtain

$$\bar{\sigma}_{k+1} = \bar{\sigma}_k + CB^*\bar{u}_k^s, \tag{58}$$

which is the discrete counterpart of (5). For the design of $\bar{u}^s$, let us choose $\bar{u}_k^s$ such that $\bar{u}^s$ steers $\bar{\sigma}_k$ to 0 in finite time. Following the work in [11] and [12], we use an implicit discretization of the continuous-time control law. The discrete-time sliding variable dynamics is given by (58) and $\bar{u}_k^s \in -\alpha \operatorname{Sgn}(\bar{\sigma}_{k+1})$. Inserting (57) in (11), the discrete-time dynamics of the nominal controlled plant is

$$\begin{cases} \bar{x}_{k+1} = (e^{Ah} + B^*(CB^*)^{-1}C(I - e^{Ah}))\bar{x}_k + B^*\bar{u}_k^s \\ \bar{\sigma}_{k+1} = \bar{\sigma}_k + CB^*\bar{u}_k^s. \end{cases}$$

Using the framework of generalized (set-valued) equations, the discrete-time sliding variable dynamics is

$$\begin{cases} \bar{\sigma}_{k+1} = \bar{\sigma}_k + CB^*\bar{u}_k^s \\ \bar{u}_k^s \in -\alpha \operatorname{Sgn}(\bar{\sigma}_{k+1}). \end{cases} \tag{59}$$

This system has the same structure as in (15), although with the important difference that we have here $\widetilde{\sigma}_{k+1} = \bar{\sigma}_{k+1}$. Therefore, we can show that $\bar{\sigma}_k$ goes to 0 in finite time, see Proposition 1 in Section 7. Hence in the nominal case, the system reaches the sliding surface at a certain time t_{k_0} and then for all $k > k_0$, $\bar{\sigma}_k = 0$.

Lemma 10. *Suppose CB^* is a* **P***-matrix. Then the only equilibrium pair of the system* (59) *is* $(\bar{\sigma}_*, \bar{u}^s_*) = (0, 0)$.

Proof. A pair $(\bar{\sigma}, \bar{u}^s)$ is an equilibrium of (59) if and only if $CB^*\bar{u}^s = 0$. If CB^* is a **P**-matrix, then it has full-rank and $CB^*\bar{u}^s = 0$ is equivalent to $\bar{u}^s = 0$. By the definition of the Sgn multifunction in (2), this is only possible if $\bar{\sigma} = 0$. □

With this scheme the two control inputs are

$$\begin{cases} \bar{u}^{eq}_k = (CB^*)^{-1} C(I - e^{Ah})\bar{x}_k \\ \bar{u}^s_k \qquad \text{solution of (59).} \end{cases} \tag{60}$$

This controller is nonanticipative since $\bar{u}^{eq}_k$ depends only on the model parameters and $\bar{x}_k$. Moreover $\bar{u}^s_k$ is the unique solution to (59) given that $CB^* > 0$, using similar arguments as in Lemma 4. This controller retains the structure of the continuous-time sliding mode controller. It is different from the approach that can be found in [4] or [21] since the equivalent part u^{eq} is not chosen as the solution to a deadbeat control problem. As a result, the magnitude of the control is of order $\mathcal{O}(1)$ with respect to the timestep h, whereas it is of order $\mathcal{O}(h^{-1})$ in the deadbeat case, see [21].

6 Simulations of a 2-dimensional system

To illustrate the results obtained with different discretization methods, let us simulate the following controlled system:

$$\begin{cases} \dot{x}(t) = Ax(t) + B\bar{u}(t) & A = \begin{pmatrix} 0 & 1 \\ 19 & -2 \end{pmatrix}, \\ \sigma = Cx & \\ \bar{u}(t) = \bar{u}^{eq}(t) + \bar{u}^s(t) & B = \begin{pmatrix} 0 \\ 1 \end{pmatrix},\ C^T = \begin{pmatrix} 1 \\ 1 \end{pmatrix}. \end{cases} \tag{61}$$

The matrix A has the eigenvalues $\lambda_1 = 3.47$ and $\lambda_2 = -5.47$. The dynamics on the sliding surface is given by $\Pi A = \begin{pmatrix} 0 & 1 \\ 0 & -1 \end{pmatrix}$, which has eigenvalues 0 and -1. Through this section, we chose $\alpha = 1$. The initial state is $(-15, 20)^T$. The first set of simulations uses a timestep 0.3 s for the control and the second one a timestep 0.03 s. The simulations run for 150 s and were carried out with the SICONOS software package [22][1]. Figures were created using Matplotlib [23]. The schemes presented in equations (13a)–(13c) are used, as well as the two schemes in equations (14a)–(14b) for the discretization of u^s, on the ZOH sampled-data version of the system (61). In Subsection 6.1, the nominal system (61) is simulated and in Subsection 6.2 a matching perturbation is added. For each set of simulations, three types of figure are shown. The first one present an overview of the trajectories of the different closed-loop systems (like Fig. 1 and 4). The next one displays some details, around the origin (Fig. 2, 5 and 7). Finally, we present plots of the different discontinuous inputs (Fig. 3, 6 and 8). Markers are also added to help visualize the position of the closed-loop system at some of the time instants t_k.

6.1 Nominal case

The trajectories for the different closed-loop systems are plotted in Fig. 1. The motion in the reaching phase depends only on the discretization method used for the equivalent control u^{eq}. It is only near the sliding manifold that the discretization method of the discontinuous control u^s plays a role. If the explicit scheme in (13a) is used for the discretization of u^{eq}, the system diverges (Fig. 1a and 1b, curves (ei) and (ee)). This sampling method can destabilize a system which is stable in continuous time. If the implicit scheme in (13b) is used for the discretization of u^{eq}, then the discretization error may not affect stability but it can induce some unexpected behaviour. As we can see in Fig. 1, curves (ii) and (ie), the trajectories are crossing the sliding manifold. This phenomenon can be explained by the following fact: let Δ_k be the discretization error on u^{eq} at time t_k. We have the recurrence equation $\bar{\sigma}_{k+1} = \bar{\sigma}_k + \Delta_k + CB^*\bar{u}^s_k$. Let us consider the implicit discretization of u^s. If $0 < \bar{\sigma}_k < CB^*$, then the system should enter the discrete-time sliding phase. However if $\Delta_k + \bar{\sigma}_k < -2CB^*$, then for any value of $\bar{u}^s_k$, $\bar{\sigma}_{k+1} < -CB^*$. Hence, due to the discretization error, $\bar{u}^s$ fails to bring $\bar{\sigma}_{k+1}$ to 0 and the trajectory of the system crosses the sliding manifold. The same happens with the explicit discretization of u^s. With the midpoint method in (13c), curves (mi) and (me), and with the new control scheme (60), curve (ex), the system state reaches the sliding manifold.

[1] `http://siconos.gforge.inria.fr`

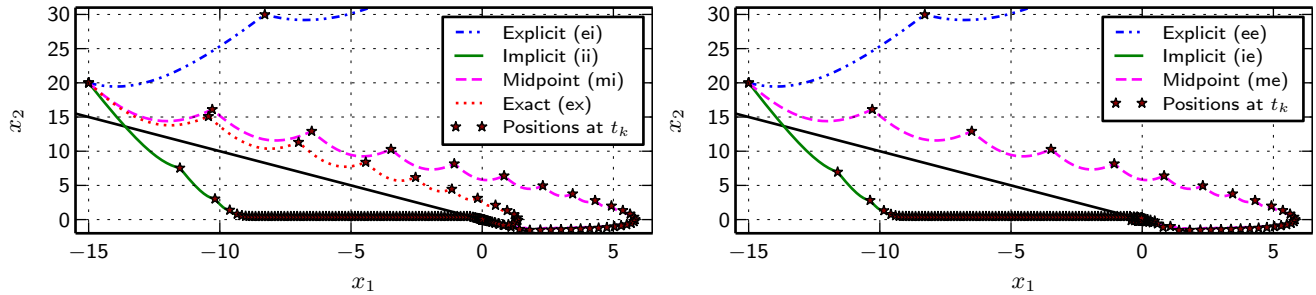

(a) Implicit discretization of u^s. (ei) is for pair (13a), (14b); (ii) for (13b), (14b); (mi) for (13c), (14b); (ex) for (60).

(b) Explicit discretization of u^s. (ee) is for pair (13a), (14a); (ie) for (13b), (14a); (me) for (13c), (14a).

Figure 1: Simulations of system (61) using different discretization methods, with $h = 0.3$ s and $\alpha = 1$.

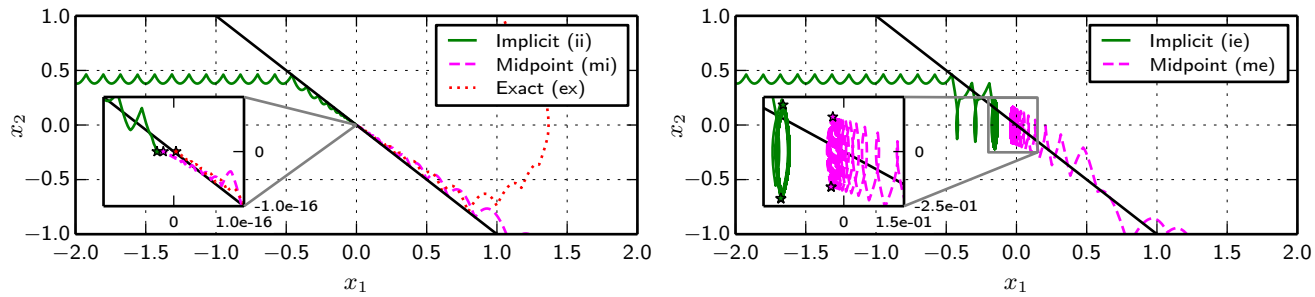

(a) Implicit discretization of u^s

(b) Explicit discretization of u^s

Figure 2: Detail of Fig. 1, $h = 0.3$ s, $\alpha = 1$.

Near the sliding manifold (Fig. 2a and 2b), the behaviour of the system is more sensitive to the discretization of u^s. In the implicit case (method (14b), Fig. 2a), in the discrete-time sliding phase, $\bar{\sigma}_k$ is very close to 0 ($\bar{\sigma}_k = 0$ with the exact method). In each case, it converges to the origin (at the machine precision). This is visible on the zoom box in Fig. 2a, where markers indicate the state of the system at each time instant t_k, during the last second of each simulation. When the explicit method (14a) is used, the system chatters around the sliding manifold, within a neighborhood of order h (0.3 s here), see Fig. 2b.

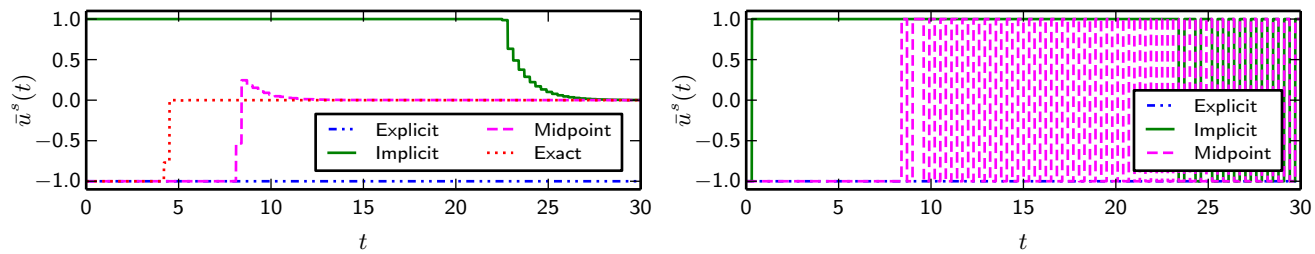

(a) Implicit discretization of u^s

(b) Explicit discretization of u^s

Figure 3: Evolution of $\bar{u}^s$ for different discretization methods, with $h = 0.3$ s and $\alpha = 1$.

In Fig. 3b, the explicitly discretized discontinuous control $\bar{u}^s$ takes its values in $\{-1, 1\}$ and starts at some point a limit cycle, as studied in [9]. This cycle is also visible on the zoom box in Fig. 2b with the help of the markers. In Fig. 3a, for each discretization of u^{eq}, $\bar{u}^s$ converges to 0, which is the value that u^s takes in the sliding phase. In the implicit and midpoint cases, at the beginning of the discrete-time sliding phase, $\bar{u}^s$ takes non zero values since there are discretization errors on u^{eq}. That is, if $\bar{\sigma}_k = 0$, $\bar{\sigma}_{k+1} \neq 0$. The discontinuous control tries to bring $\bar{\sigma}_{k+1}$ to 0 and counteracts the error. As the state goes to the origin, the error converges to 0. These simulations illustrate the fact that error is smaller in the midpoint case than in the implicit case, as shown in Lemma 7. With the exact method of Section 5, $\bar{u}^s$ goes to 0 after 1 timestep in the discrete-time sliding phase. In Fig. 3a and 3b, with the explicit discretization of u^{eq}, $\bar{u}^s$ takes always the same value, since the closed-loop system moves away from the sliding manifold. In terms of convergence to the sliding manifold, the first closed-loop system to enter the discrete-time sliding phase is the exact method (Fig. 3a), then the midpoint, finally the implicit method. With the

explicit method on u^{eq}, the system moves away from the sliding manifold and thus cannot enter the discrete-time sliding phase.

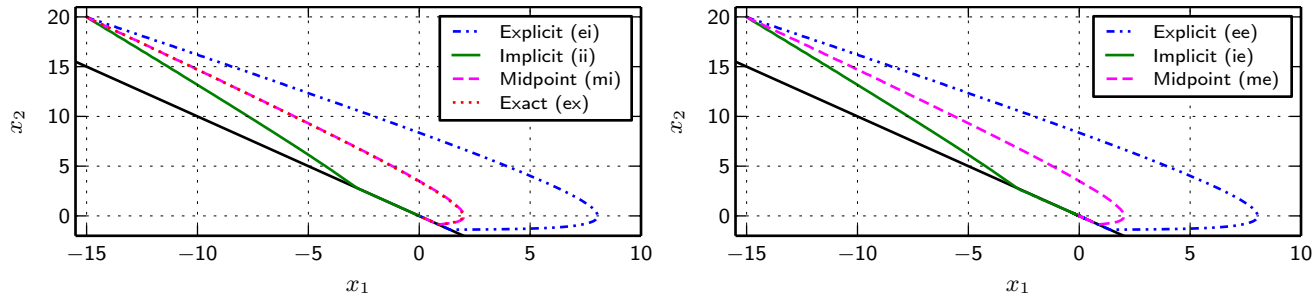

(a) Implicit discretization of u^s (b) Explicit discretization of u^s

Figure 4: Simulations of system (61) using different discretization methods, with $h = 0.03$ s and $\alpha = 1$.

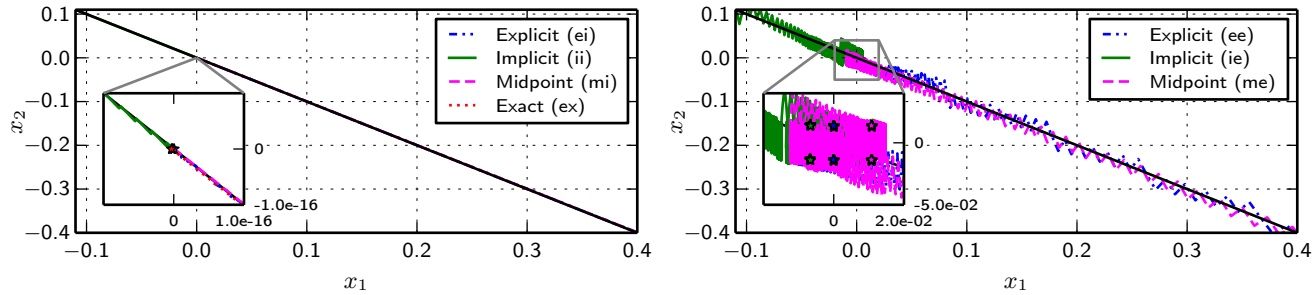

(a) Implicit discretization of u^s (b) Explicit discretization of u^s

Figure 5: Detail of Fig. 4, $h = 0.03$ s, $\alpha = 1$.

The next set of simulations uses the same parameters as the previous one, except for the timestep which is smaller: $h = 0.03$ s. In contrast with the results presented in Fig. 1, the closed-loop system is stable in all cases, see Fig. 4. As expected, the discretization error is smaller and no trajectory crosses the sliding manifold. It is not possible to distinguish the solutions associated with the midpoint from the one obtained with the exact method in Fig. 4a. In Fig. 5a with the implicit discretization of u^s, the states converge again to a very small ball near the origin. In the explicit case, there is some numerical chattering, again with the same order of magnitude as the timestep ($h = 0.03$ s, Fig. 5b). In Fig. 6a, once in the discrete-time sliding phase, $\bar{u}^s$ counteracts the discretization

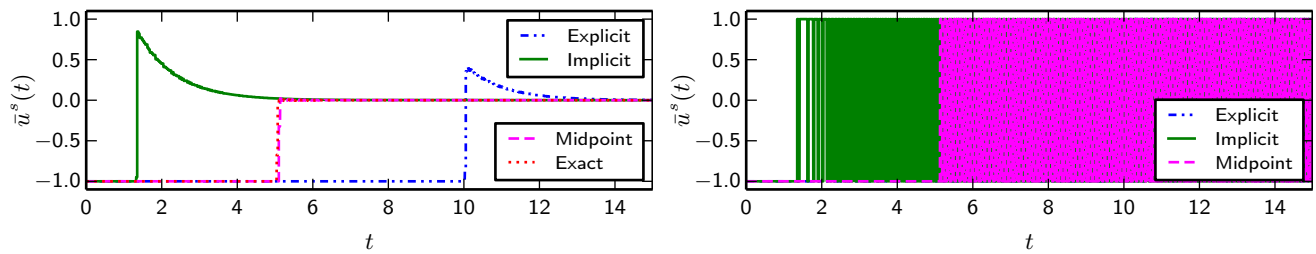

(a) Implicit discretization of u^s (b) Explicit discretization of u^s

Figure 6: Evolution of $\bar{u}^s$ for different discretization methods, with $h = 0.03$ s and $\alpha = 1$.

error on u^{eq}, which is smaller than in Fig. 3a. The discretization error for the midpoint discretization in (13c) is much smaller, and its curve overlaps completely with the one of the exact discretization method.

The results presented here bring into view the numerical chattering caused by an explicit discretization of u^s, while the implicit method is free of it. The importance of the discretization of u^{eq} is also illustrated, with the explicit method leading to a diverging system and the counterintuitive behaviour yielded by the implicit method. The exact method from Section 5 produces good results and in agreement with the theoretical results.

6.2 Perturbed case

We now add a perturbation $\xi(t)$ in the system (61). In the next set of simulations, the perturbation is $\xi(t) = 0.6\exp(\min(6-t,0))\sin(2\pi t)$. Note that for all t, $\|\xi(t)\| \leq 0.6$. This particular ξ has been chosen to highlight that if the perturbation vanishes, with the implicit discretization in (14b), $\bar{u}^s$ goes to 0, whereas in the explicit case (14a), $\bar{u}^s$ continues to switch between -1 and 1. With the implicit discretization of u^s (Fig. 7a) the closed-loop system

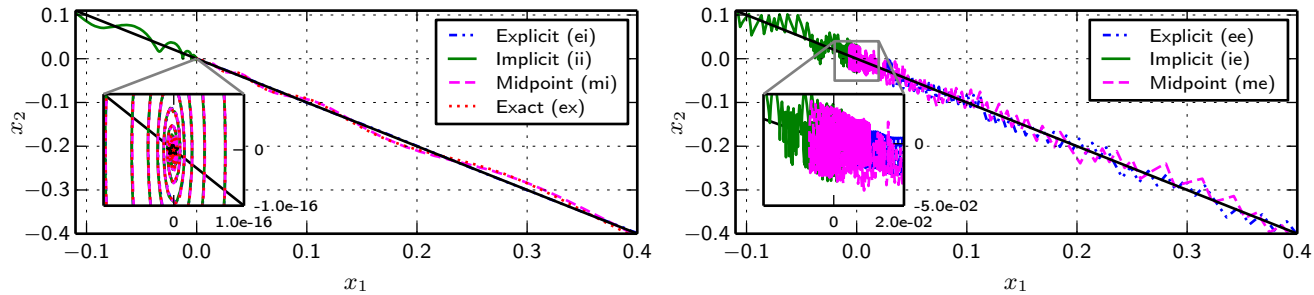

(a) Implicit discretization of u^s (b) Explicit discretization of u^s

Figure 7: Simulations of system (61) using different discretization methods for u^{eq} and $h = 0.03$ s (perturbed case).

enters the discrete-time sliding phase at some point. Then $\bar{u}^s_k = -(CB^*)^{-1}Cp_{k-1}$, if some simple assumptions are satisfied, see the proof of Proposition 2 below. It takes such value in order to counteract the effect of the perturbation during the elapsed time interval, hence imitating the continuous-time Filippov solutions. However the trajectories are now clearly only in a neighborhood of the sliding manifold. Finally in each case in Fig. 8a, $\bar{u}^s_k$ settles to 0, as in continuous time. Indeed, the perturbation ξ used in this simulation goes to 0 exponentially fast at some point. On the other hand, with an explicit discretization of u^s (Fig. 8b), it is much harder to witness the influence of the perturbation on $\bar{u}^s$ since filtering would be necessary to see the effect. The control input chattering is striking with the explicit discretization in Fig. 3b, 6b, and 8b. In Fig. 9 we further illustrate the phenomenon

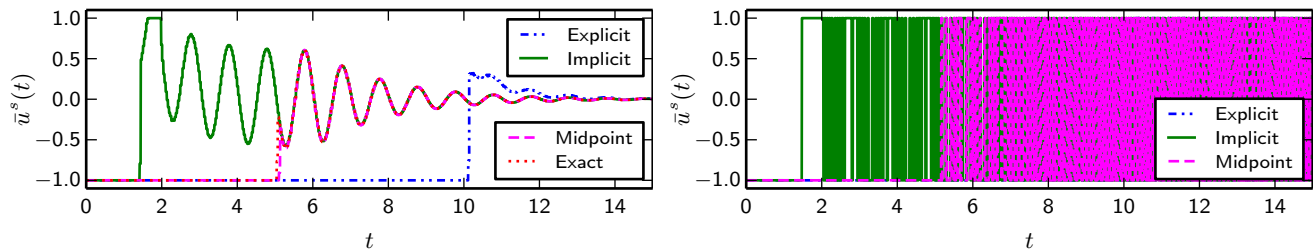

(a) Implicit discretization of u^s (b) Explicit discretization of u^s

Figure 8: Evolution of $\bar{u}^s$ for different discretization methods for u^{eq} and u^s, $h = 0.03$ s. (perturbed case)

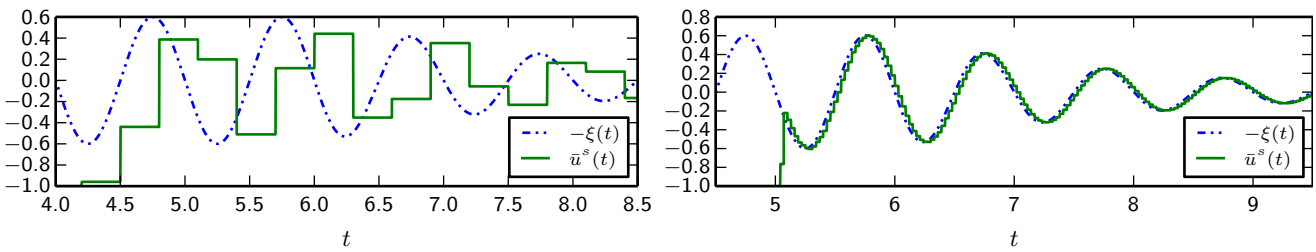

(a) $h = 0.3$ s (b) $h = 0.03$ s

Figure 9: Evolution of $\bar{u}^s$ and the perturbation using the new control scheme for two different timesteps.

in the implicit case: $\bar{u}^s$ approximates $-\xi$ with a delay depending on h. This is close to the behaviour one expects from the Filippov's framework in continuous-time. We shall investigate this phenomenon in Section 7.

The following simulation results illustrate that with an implicit discretization of u^s, the chattering in the discrete-time sliding phase is solely due to the perturbation. The setup is the same as in Section 6.1, except that there is

a perturbation $\xi(t) = 0.9\sin(t)$ and α, the magnitude of the discontinuous control, changes. For the present set of simulation, we use $\alpha = 1, 3$ and 10, values large enough to ensure that the perturbation is always dominated by the control. On Fig. 10a, we cannot distinguish the three trajectories in the discrete-time sliding phase, since even if $\bar{u}_k^s$ takes value in a larger set, the selected value within (α, α) does not change. This is supported by the Fig. 11a: it is again not possible to differentiate the values taken by the controllers. On the contrary, in Fig. 10b, the three different trajectories are clearly visible. Here we observe that the numerical chattering is dominant. Each time we increase α, the amplitudes of the oscillation around the manifold are getting bigger. We also observe that the precision of the system seems to be affected by the magnitude of the control. The bigger it is, the farther the system oscillates from the origin.

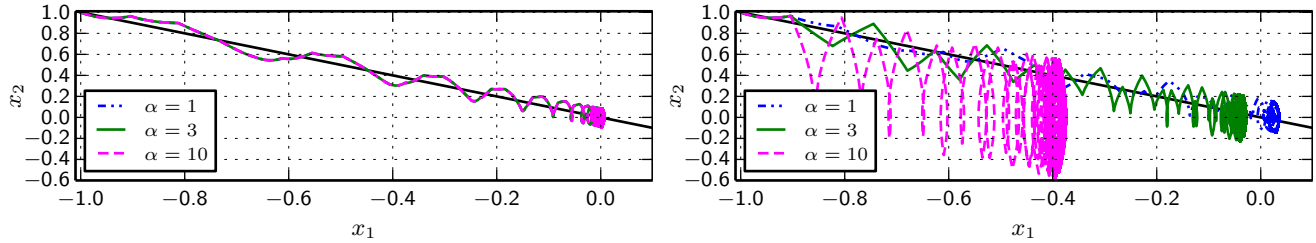

(a) Implicit discretization of u^s. (b) Explicit discretization of u^s.

Figure 10: Simulations of system (61) with a perturbation, using different values for α and with $h = 0.1$s.

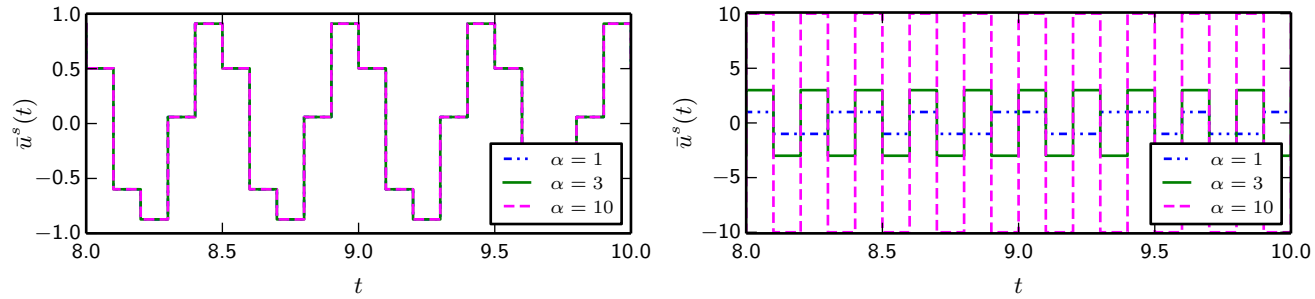

(a) Implicit discretization of u^s. (b) Explicit discretization of u^s.

Figure 11: Evolution of $\bar{u}^s$, using different values for α and with $h = 0.1$ s.

7 Stability properties

7.1 Nominal case

In this subsection, the stability of the system (59) is analyzed. Using the equivalent control proposed in Section 5, the obtained properties can be transposed to the original nominal system (1). Note that the mapping $\mathrm{Sgn}(\cdot)$, as introduced in Definition 1, has the following properties:

$$\langle v_1 - v_2, x_1 - x_2 \rangle \geq 0, \ \forall v_i \in \mathrm{Sgn}(x_i), i = 1, 2 \tag{62}$$

$$0 \notin \mathrm{Sgn}(x), \ \forall x \neq 0. \tag{63}$$

Property (62) is known as the *monotonicity* of the Sgn set-valued function. The positive-definitiveness property of CB^* is pivotal to the results presented in this section. Even if it is not explicit with the current notations, CB^* depends on the timestep h. The following lemma gives some insight of when this condition is fulfilled.

Lemma 11. *Suppose that CB is positive-definite. There exists an interval $I = [0, h^*] \subset \mathbb{R}_+$, $h^* > 0$ such that if the timestep h is chosen in I, then CB^*/h is positive-definite (and so is CB^* if $h \neq 0$).*

Proof. Let $h > 0$, CB_s and CB_s^* are the symmetric part of CB and CB^*, respectively. Let $\Delta := CB_s^*/h - CB_s = \sum_{l=1}^{\infty} \frac{CA^lB + B^T(A^l)^TC^T}{2(l+1)!} h^l = \mathcal{O}(h)$. Since CB_s is symmetric, it is also normal. Hence we can apply Corollary 4.2.16,

p. 405 in [24], which yields that for any eigenvalue μ of CB_s^*/h, $\min_\lambda |\lambda - \mu| \leq \|\Delta\|_{2,2}$, with λ an eigenvalue of CB_s and $\|\cdot\|_{2,2}$ the spectral norm. By definition, Δ is a symmetric matrix with real entries. Hence $\|\Delta\|_{2,2} = \delta_{max}$, the largest module of any eigenvalue of Δ. Let $\gamma > 0$ be the smallest eigenvalue of CB_s. If $\delta_{max} < \gamma$, then every eigenvalue of CB_s^*/h is positive and since CB_s^*/h is by definition symmetric, CB_s^*/h is positive definite. It is easy to see that $\Delta \to 0$ as $h \to 0$ and that Δ depends continuously on h. Therefore by Corollary 4.2.4, p. 399 in [24], the eigenvalues of Δ are continuous functions of h. Then it is always possible to find h^* such that $\delta_{max} < \gamma$ for all $h < h^*$, which implies that CB_s^*/h is positive-definite and finally CB_s^* is positive definite. □

Lemma 12. *If CB^* is symmetric positive-definite, then the equilibrium state $\bar{\sigma}^* = 0$ of (59) is globally Lyapunov stable.*

Proof. Let $V(\bar{\sigma}_k) := \bar{\sigma}_k^T P \bar{\sigma}_k$ with $P = (CB^*)^{-1}$, be a candidate Lyapunov function. Along the trajectories of the system (59), one obtains:

$$\begin{aligned} V(\bar{\sigma}_{k+1}) - V(\bar{\sigma}_k) &= \bar{\sigma}_{k+1}^T P \bar{\sigma}_{k+1} - \bar{\sigma}_k^T P \bar{\sigma}_k \\ &= \bar{\sigma}_{k+1}^T P \bar{\sigma}_{k+1} - (\bar{\sigma}_{k+1} - CB^* \bar{u}_k^s)^T P (\bar{\sigma}_{k+1} - CB^* \bar{u}_k^s) \\ &= -(\bar{u}_k^s)^T CB^* \bar{u}_k^s + 2(\bar{u}_k^s)^T \bar{\sigma}_{k+1}. \end{aligned} \tag{64}$$

Using (62) with $v_1 = \bar{u}_k^s$, $v_2 = 0$, $x_1 = \bar{\sigma}_{k+1}$, and $x_2 = 0$ yields $(\bar{u}_k^s)^T \bar{\sigma}_{k+1} \leq 0$. Since CB^* is positive-definite, the first term is always nonpositive. This completes the proof. □

We can also use a non-quadratic Lyapunov function, inspired by the one presented in [25]. As we shall see, it relaxes the symmetry condition on the matrix CB^*.

Lemma 13. *If CB^* is positive-definite, then the equilibrium state $\bar{\sigma}^* = 0$ of (59) is globally Lyapunov stable.*

Proof. Let $V(\bar{\sigma}_k) := -(\bar{u}_{k-1}^s)^T \bar{\sigma}_k$ be the candidate Lyapunov function, and $\bar{u}_{k-1}^s \in -\alpha \operatorname{Sgn}(\bar{\sigma}_k)$. The function V is positive definite, radially unbounded, and decrescent since $-(\bar{u}_{k-1}^s)^T \bar{\sigma}_k = \alpha \|\bar{\sigma}_k\|_1^2$ and $\alpha > 0$. Let us study the variations of V:

$$\begin{aligned} V(\bar{\sigma}_{k+1}) - V(\bar{\sigma}_k) &= -(\bar{u}_k^s)^T \bar{\sigma}_{k+1} + (\bar{u}_{k-1}^s)^T \bar{\sigma}_k \\ &= -(\bar{u}_k^s)^T (\bar{\sigma}_k + CB^* \bar{u}_k^s) + (\bar{u}_{k-1}^s)^T \bar{\sigma}_k \\ &= -(\bar{u}_k^s)^T CB^* \bar{u}_k^s + \langle \bar{u}_{k-1}^s - \bar{u}_k^s, \bar{\sigma}_k \rangle. \end{aligned} \tag{65}$$

The first term is always nonpositive with the hypothesis on CB^*. For the second term, if $\bar{u}_k^s \in -\alpha \operatorname{Sgn}(\bar{\sigma}_{k+1})$, then it also belongs to $-\alpha \operatorname{Sgn}(0)$. Hence, by (62), the second term is always nonpositive. This completes the proof. □

Proposition 1. *If the hypothesis of either Lemma 12 or 13 are satisfied, then the fixed point $(\bar{\sigma}, \bar{u}) = (0, 0)$ of (59) is globally finite-time Lyapunov stable.*

Proof. In each case, the difference $V(\bar{\sigma}_{k+1}) - V(\bar{\sigma}_k)$ consists of $-(\bar{u}_k^s)^T CB^* \bar{u}_k^s$ plus a nonpositive term. Since CB^* is positive-definite, it holds that $-(\bar{u}_k^s)^T CB^* \bar{u}_k^s \leq -\beta \|\bar{u}_k^s\|^2$, with $\beta > 0$ the smallest eigenvalue of CB_s^*. Note that if $\bar{\sigma}_{k+1} \neq 0$, then $\|\bar{u}_k^s\| \geq \alpha$ and $V(\bar{\sigma}_{k+1}) - V(\bar{\sigma}_k) \leq -\alpha^2 \beta$. Iterating, one obtains $V(\bar{\sigma}_{k+1}) - V(\bar{\sigma}_0) \leq -k\alpha^2\beta$. Let $k_0 := \lceil V(\bar{\sigma}_0)/\beta\alpha^2 \rceil$. Suppose $V(\bar{\sigma}_{k_0+1}) \neq 0$. Then $V(\bar{\sigma}_{k_0+1}) - V(\bar{\sigma}_0) \leq -k_0\alpha^2\beta \leq -V(\bar{\sigma}_0)$. This yields $V(\bar{\sigma}_{k_0+1}) \leq 0$, which implies $V(\bar{\sigma}_{k_0+1}) = 0$. Then $\bar{\sigma}_{k_0+1} = 0$ and $\bar{\sigma}_k = 0$ for all $k > k_0$. □

7.2 Perturbed case

Let us now consider the case with perturbation. The evolution of the sliding variable $\bar{\sigma}$ is governed by

$$\bar{\sigma}_{k+1} = \bar{\sigma}_k + CB^* \bar{u}_k^s + Cp_k, \tag{66}$$

where $p_k := \int_{t_k}^{t_{k+1}} e^{A(t_{k+1}-\tau)} B\xi(\tau) \mathrm{d}\tau$ and $\bar{u}_k^s$ is the unique solution of the generalized equation (15). Although the system will never reach and stay on the sliding manifold as in the continuous-time case, it enters the discrete-time sliding phase as stated in Definition 4 and stays in it. Let us first present a technical lemma.

Lemma 14. *Let $M \in \mathbb{R}^{n\times n}$ and $M_s := 1/2(M + M^T)$. Suppose M is positive-definite. Let $\beta > 0$ be the smallest eigenvalue of M_s. Then for all $x \in \mathbb{R}^n$, $\|M^{-1}x\| \leq \beta^{-1}\|x\|$.*

Proof. M^{-1} exists since M_s is positive-definite. Let ν_{min} (resp. ν_{max}) be the smallest (resp. largest) singular values of M (resp. M^{-1}). Two relations hold: $\nu_{max} = \nu_{min}^{-1}$ [26, Fact 6.3.21, p.233] and $\nu_{min} \geq \beta > 0$ [27, Corollary 3.1.5, p.151]. Then using the spectral norm definition, $\|M^{-1}x\| \leq \|M^{-1}\|\|x\| = \nu_{max}\|x\| \leq \beta^{-1}\|x\|$. □

From now on, let $CB_s^* := 1/2(CB^* + (CB^*)^T)$ and let β be its smallest eigenvalue.

Proposition 2. *Suppose that CB^* is positive-definite. If $\alpha > 0$ is such that for all $k \in \mathbb{N}$ $\|Cp_k\| < \alpha\beta$, then the perturbed closed-loop system* (66)-(15) *will enter the discrete-time sliding phase in finite time and stay in it. Furthermore if $h \in [0, h^*]$, as defined in Lemma 11, then there exists an upper bound T^* on the duration of the reaching phase.*

Proof. Let $V(\bar{\sigma}_k) := -\bar{u}_{k-1}^{sT}\bar{\sigma}_k$, $\bar{u}_{k-1}^s \in -\alpha\,\mathrm{Sgn}(\bar{\sigma}_k)$. Assume that the system is initialized outside the discrete-time sliding phase. From Definition 4, it follows that $\|\bar{u}_k^s\| \geq \alpha$. Starting from (65), doing as in the proof of Proposition 1 and adding the contribution of the perturbation, we have $V(\bar{\sigma}_{k+1}) - V(\bar{\sigma}_k) \leq -\beta\|\bar{u}_k^s\|^2 - (\bar{u}_k^s)^T Cp_k$. Using the Cauchy-Schwarz inequality, we obtain $|(\bar{u}_k^s)^T Cp_k| \leq \|\bar{u}_k^s\|\|Cp_k\|$. To ensure that V decreases strictly, we need $\|Cp_k\| < \beta\|\bar{u}_k^s\|$. This condition is satisfied using the hypothesis on the gain α and the fact that $\beta > 0$. Note that even in the case with multiple switching surfaces, V decreases as long as the system is not "sliding" on the intersection of all the manifolds. If $\widetilde{\sigma}_{k+1} = 0$, then we enter the discrete-time sliding phase. The finite-time property is derived as in the proof of Proposition 1. Let $\kappa = \alpha\beta - \|Cp_k\|$. From the assumption, $\kappa > 0$ holds. In the reaching phase, V decreases by at least $\kappa\alpha$ at each timestep. Hence, $V(\bar{\sigma}_k)$ converges to 0 in finite-time. Now if the system is in the discrete-time sliding phase at t_k, then $\widetilde{\sigma}_{k+1} = 0$ and $\bar{\sigma}_{k+1} = Cp_k$. At time t_{k+1}, we have $\widetilde{\sigma}_{k+2} = Cp_k + CB^*\bar{u}_{k+1}^s$. Let us show that $\bar{u}_{k+1}^s = -(CB^*)^{-1}Cp_k$ is the unique solution to the generalized equation (15). With this value, $\widetilde{\sigma}_{k+2} = 0$. Using Lemma 14 and the hypothesis, $\|\bar{u}_{k+1}^s\| \leq \beta^{-1}\|Cp_k\| < \alpha$. Relations between norms yield $\|\bar{u}_{k+1}^s\|_\infty < \alpha$. Then $\bar{u}_{k+1}^s \in (\alpha, \alpha)^p \subset \alpha\,\mathrm{Sgn}(0)$ and $\bar{u}_{k+1}^s$ is a solution to (15). With the hypothesis of the proposition, CB^* is also a **P**-matrix. Then Lemma 4 can be applied and yields the uniqueness property. Thus $\bar{u}_{k+1}^s = -(CB^*)^{-1}Cp_k$ is the unique solution to (15) at time t_{k+1}, and by induction, the system stays in the discrete-time sliding phase.

In the following, we suppose that $0 < h < h^*$. Let $\delta_{max}^* = \|\Delta\|_{2,2}$ when $h = h^*$. From the expression of k_0 in the proof of Proposition 1, the duration of the reaching phase is $hk_0 < \frac{V(\bar{\sigma}_0)h}{\beta\alpha^2} + h$. Note that β/h is an eigenvalue of CB_s^*/h. Applying again Corollary 4.2.16, p. 405 in [24], we have $\lambda - \beta/h \leq \delta_{max} \leq \delta_{max}^*$, with λ an eigenvalue of CB_s. This yields $\gamma - \delta_{max}^* \leq \lambda - \delta_{max}^* \leq \beta/h$. Using this in the previous inequality, we get $hk_0 < \frac{V(\bar{\sigma}_0)}{\alpha^2(\gamma - \delta_{max}^*)} + h^* =: T^*$. □

Remark 2. In continuous time, the condition commonly found is $\alpha > \|\xi\|_{\infty,\mathbb{R}_+}$. If the perturbation ξ is continuous, then it is possible to link this condition to the one used in the previous theorem, $\|Cp_k\| < \alpha\beta$ for all $k \in \mathbb{N}$. Using the mean value theorem for integration, we get $Cp_k = hCe^{A(t_{k+1}-t')}B\xi(t') = hCB\xi(t') + \mathcal{O}(h^2)$, with $t' \in [t_k, t_{k+1}]$. Hence the first-order estimation for $\|Cp_k\|$ is $h\|CB\|_{2,2}\|\xi\|_2 \leq \|CB\|_{2,2}\sqrt{p}\|\xi\|_\infty$. From the proof of Lemma 11, we have $\beta = h\lambda_{min}(CB) + \mathcal{O}(h^2)$. Then we get $\alpha > \|CB\|_{2,2}\sqrt{p}\|\xi\|_\infty/\beta + \mathcal{O}(h)$. Note that $\|CB\|_{2,2} > \lambda_{max}(CB)$ [27, Corollary 3.1.5, p.151]. Therefore $\|CB\|_{2,2}\sqrt{p}\|\xi\|_\infty/\beta \geq 1$ and for h small enough, $\|Cp_k\| < \alpha\beta$ implies $\alpha > \|\xi\|_{\infty,\mathbb{R}_+}$. If the sliding variable is a scalar, then the converse is also true at the limit.

In the classical literature on discrete-time sliding mode, dealing with the explicit discretization (14a) [1,3,7], two conditions related to the sliding variable emerged: $(\bar{\sigma}_{k+1} - \bar{\sigma}_k)_i(\sigma_k)_i < 0$ for all $i = 1, \ldots, n$, which is necessary; and the second one is $|(\bar{\sigma}_{k+1})_i| < |(\bar{\sigma}_k)_i|$. The conditions for linear systems, stated in Lemma 12, 13, and Proposition 2 are directly on the system parameters and not on the evolution on the sliding variable, which derives from the dynamics. This fact is, in our sense, much closer to the stability results obtained in continuous-time [25].

Let us now turn our attention to the relationship between u and $\bar{u}$. In particular, we study the convergence of $\bar{u}$ to u during the discrete-time sliding phase, which is established after $T^* < +\infty$.

Proposition 3. *Consider the discrete-time closed-loop system given by* (66) *and* (15). *Let $\{h_n\}_{n\in\mathbb{N}}$ be any strictly decreasing sequence of positive numbers converging to* 0 *and with $h_0 < h^*$ (see Lemma 11). Suppose that the perturbation $\xi\colon \mathbb{R} \to \mathbb{R}^p$ is uniformly continuous, that CB is positive-definite and that $\alpha > 0$ is chosen such that the conditions of Proposition 2 are satisfied for each timestep h_n. Then for any $S \subseteq [T^*, \infty)$, $\lim_{h_n\to 0}\|\bar{u}^s - u^s\|_{\infty,S} = 0$.*

Proof. Let $\{t_k\}$ be a sequence such that for all $k \in \mathbb{N}$, $t_{k+1} - t_k = h_n$. For the sake of clarity, we omit to write explicitly the dependence on n. From Proposition 2 and Lemma 11, we know that for all k such that $t_k \geq T^*$, $\bar{u}_k^s = -(CB^*)^{-1}Cp_{k-1} = -(CB^*)^{-1}C\int_{t_{k-1}}^{t_k} e^{A(t_k-\tau)}B\xi(\tau)\mathrm{d}\tau$. During the sliding phase, the continuous-time controller satisfies $u^s(t) = -\xi(t)$. Let S be any time interval contained in $[T^*, +\infty)$. Let $t \in S$ and $k \in \mathbb{N}$ is

such that $t \in [t_k, t_{k+1})$. Hence $\bar{u}^s(t) = \bar{u}^s_k$. Let us study $\bar{u}^s_k - u^s(t)$:

$$\bar{u}^s_k - u^s(t) = -(CB^*)^{-1} C \int_{t_{k-1}}^{t_k} e^{A(t_k-\tau)} B\xi(\tau)\mathrm{d}\tau + \xi(t) \tag{67}$$

$$= -(CB^*)^{-1} \left(\int_{t_{k-1}}^{t_k} Ce^{A(t_k-\tau)} B\xi(\tau)\mathrm{d}\tau - CB^*\xi(t) \right). \tag{68}$$

Using (12), we obtain:

$$\bar{u}^s_k - u^s(t) = -(CB^*)^{-1} \left(\int_{t_{k-1}}^{t_k} Ce^{A(t_k-\tau)} B\xi(\tau)\mathrm{d}\tau - \int_{t_k}^{t_{k+1}} Ce^{A(t_{k+1}-\tau)} B\xi(t)\mathrm{d}\tau \right). \tag{69}$$

With the change of variable $\tau' = \tau + h_n$ in the first integral, we can group the two integrals in (69) as follows:

$$\bar{u}^s_k - u^s(t) = -(CB^*)^{-1} \left(\int_{t_k}^{t_{k+1}} Ce^{A(t_{k+1}-\tau)} B(\xi(\tau - h_n) - \xi(t)\mathrm{d}\tau \right) \tag{70}$$

$$= -(CB^*)^{-1} \left(\int_{t_k}^{t_{k+1}} CB(\xi(\tau - h_n) - \xi(t)) + \sum_{l=1}^{\infty} \frac{CA^l B}{l!} \left((t_{k+1} - \tau)^l (\xi(\tau - h_n) - \xi(t)) \right) \mathrm{d}\tau \right). \tag{71}$$

Using again (12), let us provide an approximation for the first factor:

$$(CB^*)^{-1} = \left(h_n CB + \sum_{l=1}^{\infty} \frac{CA^l B}{(l+1)!} h_n^{l+1} \right)^{-1} \tag{72}$$

$$= \left(I + \sum_{l=1}^{\infty} \frac{(CB)^{-1} CA^l B}{(l+1)!} h_n^l \right)^{-1} (h_n CB)^{-1} \tag{73}$$

$$= \left(I - \frac{(CB)^{-1} CAB}{2} h_n + \mathcal{O}(h_n^2) \right) (h_n CB)^{-1}. \tag{74}$$

The Taylor expansion holds if $\sum_{l=1}^{\infty} \frac{(CB)^{-1} CA^l B}{(l+1)!} h_n^l$ has all its eigenvalues in the unit disk. This is a mere technical restriction, since it is always possible to find a small enough positive number h_{n_0} such this condition is satisfied. Since we are interested in the case where $\{h_n\}$ converges to 0, this requirement is supposed to hold. For the first term in the integrand in (71), we apply the mean value theorem for integration. If ξ is a vector-valued function (this is the case when the sliding variable has dimension greater than 1), we apply the theorem for each component separately. This yields for $i = 1, \ldots, n$ $(\int_{t_k}^{t_{k+1}} \xi(\tau - h_n) - \xi(t)\mathrm{d}\tau)_i = h_n(\xi_i(t'_i - h_n) - \xi_i(t))$ for some $t'_i \in [t_k, t_{k+1}]$. For the second part of the integrand in (71), we exchange the summation and integral signs. This is possible since the matrix exponential converges normally and ξ is bounded on any interval $[t_k, t_{k+1}]$ (ξ is continuous). Moreover for all $l \geq 1$, with $\tau \in [t_k, t_{k+1}]$, $(t_{k+1} - \tau)^l \xi(\tau - h_n) - \xi(t)) = \mathcal{O}(h_n)$. Thus $\int_{t_k}^{t_{k+1}} (t_{k+1} - \tau)^l (\xi(\tau - h_n) - \xi(t))\mathrm{d}\tau = \mathcal{O}(h_n^2)$. Then (71) can be rewritten as:

$$\bar{u}^s_k - u^s(t) = -(I + \mathcal{O}(h_n)) \left(\int_{t_k}^{t_{k+1}} h_n^{-1} (\xi(\tau - h_n) - \xi(t))\mathrm{d}\tau + \mathcal{O}(h_n) \right). \tag{75}$$

Taking the supremum norm yields:

$$\|\bar{u}^s_k - u^s(t)\|_\infty \leq \|I + \mathcal{O}(h_n))\|_\infty \left(\max_i \sup_{t \in [t_k, t_{k+1}]} |\xi_i(t'_i - h) - \xi_i(t)| + \|\mathcal{O}(h_n)\|_\infty \right) \tag{76}$$

$$\leq \max_i \sup_{t \in [t_k, t_{k+1}]} |\xi_i(t'_i - h_n) - \xi_i(t)| + \mathcal{O}(h_n). \tag{77}$$

Since ξ is uniformly continuous, for every $\varepsilon > 0$, there exists $\delta > 0$ such that for all $t_1, t_2 \in \mathbb{R}$, $|t_1 - t_2| \leq \delta$ implies $\|\xi(t_1) - \xi(t_2)\| \leq \varepsilon$. Then the right-hand side of (77) is converging to 0 as $h_n \to 0$. Since this is true for all $t \in S$, the proof is complete. □

It is also interesting to study the convergence of the variation of the control variable, which may be thought of as a measure of the control input chattering. Let us first define the variation of a function in some special cases. The material in Definitions 5 and 6 is adapted from [28].

Definition 5. Let $f\colon \mathbb{R} \to \mathbb{R}^m$ be a right-continuous step function, discontinuous at finitely many time instants t_k and $t_0, T \in \mathbb{R}$, $t_0 < T$. Then the variation of f on $[t_0, T]$ is defined as:

$$\mathrm{Var}_{t_0}^{T}(f) := \sum_k \|f(t_k) - f(t_{k-1})\|, \tag{78}$$

with $k \in \mathbb{N}$ such that $t_k \in (t_0, T]$.

Definition 6. Let $f\colon \mathbb{R} \to \mathbb{R}^m$ be a continuously differentiable function, with bounded derivatives and let $t_0, T \in \mathbb{R}$, $t_0 < T$. Then the variation of f on $[t_0, T]$ is defined as:

$$\mathrm{Var}_{t_0}^{T}(f) := \int_{t_0}^{T} \|\dot{f}(\tau)\| \mathrm{d}\tau. \tag{79}$$

Proposition 4. *Let $\{h_n\}_{n\in\mathbb{N}}$ be any strictly decreasing sequence of positive numbers converging to 0 with $h_0 < h^*$. Suppose that CB is positive-definite, and ξ is a real-valued continuously differentiable with bounded derivative function. Let α be chosen such that the conditions of Proposition 2 are verified for each h_n. Then $\lim_{h_n\to 0} \mathrm{Var}_{T^*}^{T}(\bar{u}^s) = \mathrm{Var}_{T^*}^{T}(u^s)$.*

Proof. Let $\{t_k\}$ be a sequence such that for all $k \in \mathbb{N}$, $t_{k+1} - t_k = h_n$. Let us recall that, with the implicit controller defined in Equations (66) and (15), the reaching phase duration is bounded and that the sliding phase is established at $t = T^*$ if h is small enough. Let $\mathrm{Var}_{T^*}^{T}(\bar{u}^s)$ denote the variation of the function $\bar{u}^s$ on the time interval $[T^*, T]$. The variation of the step function $\bar{u}^s$ is:

$$\mathrm{Var}_{t_0}^{T}(\bar{u}^s) = \sum_k \|\bar{u}^s_{k+1} - \bar{u}^s_k\| = \sum_k \|(CB^*)^{-1}C \int_{t_k}^{t_{k+1}} e^{A(t_{k+1}-\tau)} B\xi(\tau)\mathrm{d}\tau - (CB^*)^{-1}C \int_{t_{k-1}}^{t_k} e^{A(t_k-\tau)} B\xi(\tau)\mathrm{d}\tau\| \tag{80}$$

$$= \sum_k \|(CB^*)^{-1} \left(\int_{t_k}^{t_{k+1}} CB(\xi(\tau) - \xi(\tau - h_n))\mathrm{d}\tau + \int_{t_k}^{t_{k+1}} C(e^{A(t_{k+1}-\tau)} - I)B(\xi(\tau) - \xi(\tau - h_n)) \right) \|. \tag{81}$$

Using the approximation for $(CB^*)^{-1}$ obtained in (74), we get:

$$\mathrm{Var}_{t_0}^{T}(\bar{u}^s) \le (I + \mathcal{O}(h_n)) \sum_k \| \int_{t_k}^{t_{k+1}} \frac{\xi(\tau) - \xi(\tau - h_n)}{h_n} \mathrm{d}\tau\| \tag{82}$$

$$+ (I + \mathcal{O}(h_n)) \sum_k \|(CB)^{-1} \int_{t_k}^{t_{k+1}} C(e^{A(t_{k+1}-\tau)} - I)B \frac{\xi(\tau) - \xi(\tau - h_n)}{h_n} \mathrm{d}\tau\| \tag{83}$$

$$\le (I + \mathcal{O}(h_n)) \int_{t_0}^{T} \| \frac{\xi(\tau) - \xi(\tau - h_n)}{h_n} \| \mathrm{d}\tau \tag{84}$$

$$+ (I + \mathcal{O}(h_n)) \sum_k \|(CB)^{-1} \int_{t_k}^{t_{k+1}} C(e^{A(t_{k+1}-\tau)} - I)B \frac{\xi(\tau) - \xi(\tau - h_n)}{h_n} \mathrm{d}\tau\|. \tag{85}$$

Using standard estimation inequalities, we obtain the following estimation for all integrals in the sum:

$$\| \int_{t_k}^{t_{k+1}} C(e^{A(t_{k+1}-\tau)} - I)B \frac{\xi(\tau) - \xi(\tau - h_n)}{h_n} \mathrm{d}\tau\| \le \int_{t_k}^{t_{k+1}} \|C\|\|B\|(e^{\|A\|h_n} - 1)\| \frac{\xi(\tau) - \xi(\tau - h_n)}{h_n} \| \mathrm{d}\tau. \tag{86}$$

Then we can group the terms in (85) as:

$$\mathrm{Var}_{t_0}^{T}(\bar{u}^s) \le (I + \mathcal{O}(h_n)) \int_{t_0}^{T} \| \frac{\xi(\tau) - \xi(\tau - h_n)}{h_n} \| \mathrm{d}\tau$$
$$+ (I + \mathcal{O}(h_n)) \|(CB)^{-1}\| \int_{t_0}^{T} \|C\|\|B\|(e^{\|A\|h_n} - 1)\| \frac{\xi(\tau) - \xi(\tau - h_n)}{h_n} \| \mathrm{d}\tau. \tag{87}$$

Since ξ is continuously differentiable, $\int_{t_0}^{T} \| \frac{\xi(\tau) - \xi(\tau - h_n)}{h_n} \| \mathrm{d}\tau$ converges to $\int_{t_0}^{T} \|\dot{\xi}(\tau)\| \mathrm{d}\tau = \mathrm{Var}_{t_0}^{T}(u^s)$ as $h_n \to 0$. All the other terms in the right-hand side of (87) converge to 0 as $h_n \to 0$. □

7.3 Comparison with saturated SMC

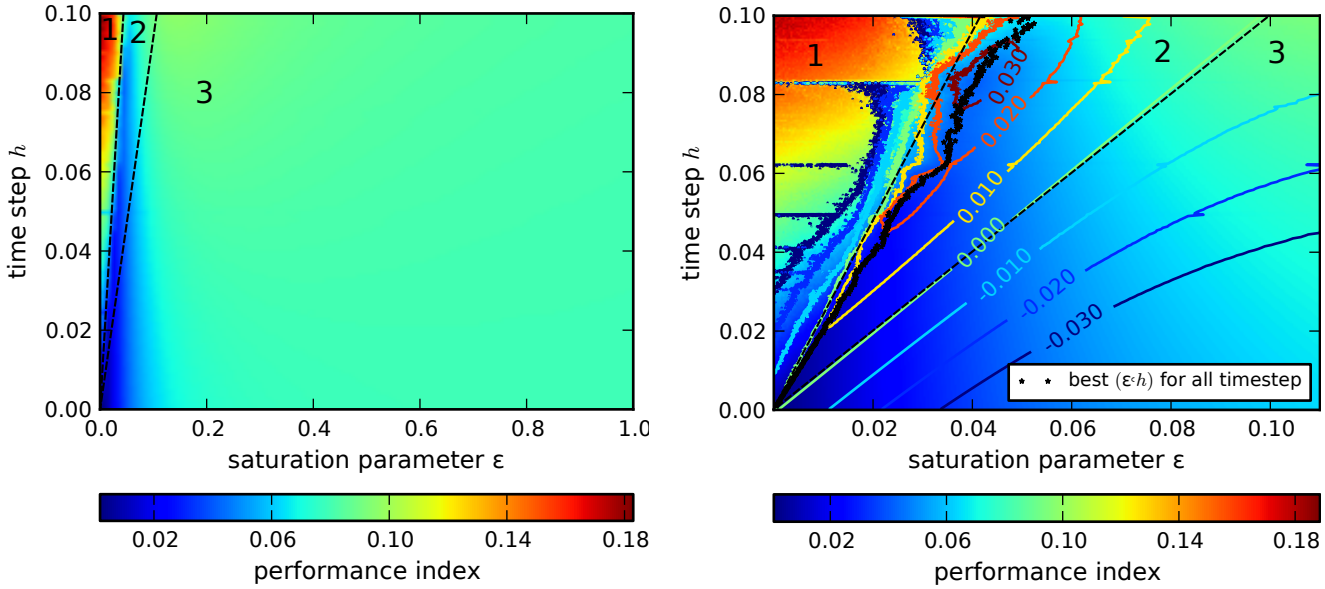

(a) Simulation results with 100 regularly spaced values for the timestep h and 100 logarithmically spaced values for the saturation parameter ε.

(b) Detail of Fig. 12a, 300 values for h and 1000 values for ε, forming a regular grid. Level sets were also added to show the difference in performance between the implicit discretization and the explicit one with saturation. If the difference is positive, the explicit saturated control is performing better than the implicit one.

Figure 12: Simulation results of a perturbed system controlled using sliding mode with a saturation. The performance index is the sum of the $|\sigma_k|$ for the last 20s.

We simulate the system (61) with a perturbation $\xi(t) = \sin 4\pi t$. Instead of using a discontinuous control, we use the following input: $u^s(t) = -\operatorname{sat}_\varepsilon(\sigma(t))$ with $\operatorname{sat}_\varepsilon(x) = \begin{cases} x/\varepsilon & \text{if } |x| \le \varepsilon \\ \operatorname{sgn}(x) & \text{if } |x| > \varepsilon \end{cases}$. As in Section 6, each simulation lasts 150s. We use two metrics to measure the performance of the different controllers. To measure the (output) chattering, due to the discretization and the perturbation, we sum the absolute value of the sliding variable $\bar{\sigma}_k$ for the last 20s: $C_1 := \sum_k |\bar{\sigma}_k|$. To measure the control effort (or input chattering), we measure the variation of the control for the last 20s: $C_2 := \operatorname{Var}_{T-20}^{T}(\bar{u}^s)$. Each quantity defines the performance index in Fig. 12 or 13. We choose to consider only the last 20s of each simulation to capture the behaviour near the sliding manifold. Let us recall that without perturbation, the implicit controller always supersedes the saturated explicit one, since it suppresses numerical chattering and $\bar{u}_k^s = 0$ in the discrete-time sliding phase. With both index, we can divide the space into 3 cones, numbered 1, 2 and 3 in Fig. 12 and 13. This separation helps us to compare both controllers. In Fig. 12a the performance in term of chattering is presented. For large values of ε, the chattering does not change when the timestep varies: the control action does not attenuate the effect of the perturbation. With a small ε, the behaviour is richer, as depicted in Fig.12b. On Fig. 12b, the overall best performance is obtained with small values for both ε and h. However for small values of ε, the performance can degrade rapidly if the sampling period h is not small enough, as seen in region 1. The dark points indicate for each value of h the pair (ε, h) of parameters yielding the best performance. It seems that there is a linear relationship between those values. However it is unclear if this observation on one particular system remains valid with a different perturbation. The level sets in Fig. 12b are used to compare the performance of the implicit and the saturated explicit controllers. On Fig. 13, the performance in terms of control cost is presented. The best performance is achieved for large ε since the slope of the saturated function is gentle. On the other hand in Fig. 13b, with a small ε, the cost increases and explodes with ε close to 0, as in region 1. The level sets indicate the difference between the costs of the 2 different controllers. It is worth noting that on region 2 where the saturated controller is better in Fig. 12b, it has a higher cost in term of control (Fig. 13b). In region 3, where the saturated controller performs less in terms of chattering (Fig. 12a), it has a smaller cost in terms of control (Fig. 13a). Indeed with a large ε, the control input is small when the closed-loop

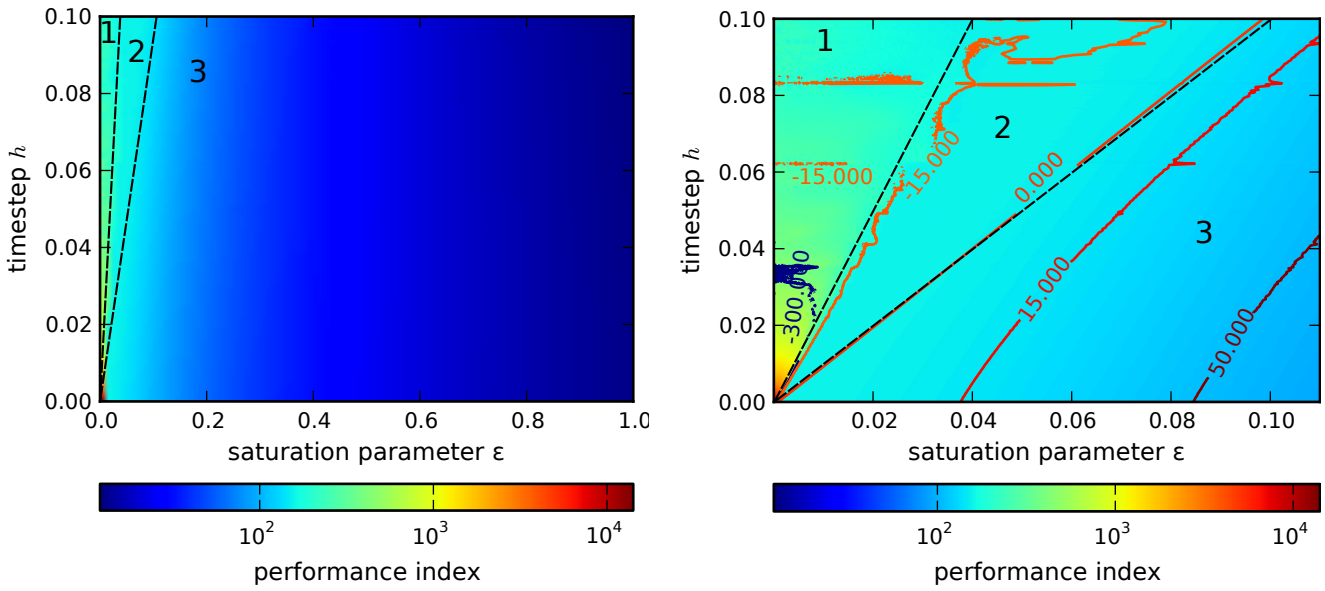

(a) Simulation results with 100 regularly spaced values for the timestep h and 100 logarithmically spaced values for the saturation parameter ε.

(b) Detail of Fig. 13a, 300 values for h and 1000 values for ε, forming a regular grid. Level sets were also added to show the difference in performance between the implicit discretization and the explicit one with saturation. If the difference is positive, the explicit saturated control is performing better than the implicit one.

Figure 13: Simulation results of the same perturbed system controlled using sliding mode with a saturation. The performance index is the sum of the $|\bar{u}^s_{k+1} - \bar{u}^s_k|$ for the last 20s.

system is close to the sliding manifold. The cost is then very small, but the disturbance is not attenuated at all. The implicit controller appeals to us as the best compromise between the input and output chattering. It is also very easy to use, since it requires no particular tuning with respect to the timestep or the perturbation.

8 Conclusion

In this article several time discretizations of the classical ECB-SMC method are analysed, from the point of view of their ability to alleviate or suppress the numerical chattering, and to guarantee the finite-time reachability of the sliding surface. A new discrete-time sliding mode control scheme is also proposed. The analysis is led from analytical estimations, as well as numerical simulations obtained with the INRIA software package SICONOS. In particular the influence of the discretization method of the state-continuous equivalent controller is studied, as well as the one of the discontinuous part of the input (explicit versus implicit discretizations). The nominal and perturbed cases are considered. The simulation results indicate that the use of an explicit discretization for the discontinuous part of the input yields numerical chattering. This is not the case when using an implicit discretization. We also provide an example where the use of an explicit discretization of u^{eq} makes the closed-loop system diverge, whereas with the other methods it attains the sliding surface. The issues related to the Lyapunov stability of the discrete-time sliding variable are also studied, using the monotonicity properties of the underlying discontinuous (set-valued) controller. Further works will include conducting experimental studies and also improvements in the perturbation attenuation.

Bibliography

References

[1] S. Sarpturk, Y. Istefanopulos, and O. Kaynak, "On the stability of discrete-time sliding mode control systems," *Automatic Control, IEEE Transactions on*, vol. 32, no. 10, pp. 930–932, 1987.

[2] S. Drakunov and V. Utkin, "On discrete-time sliding modes," in *Proc. of* IFAC *Nonlinear Control System Design Conf.*, 1989, pp. 273–278.

[3] K. Furuta, "Sliding mode control of a discrete system," *Systems & Control Letters*, vol. 14, no. 2, pp. 145–152, 1990.

[4] V. Utkin, "Sliding mode control in discrete-time and difference systems," in *Variable Structure and Lyapunov Control*, ser. Lecture Notes in Control and Information Sciences. Springer, 1994, vol. 193, pp. 87–107.

[5] W. Gao, Y. Wang, and A. Homaifa, "Discrete-time variable structure control systems," *Industrial Electronics, IEEE Transactions on*, vol. 42, no. 2, pp. 117–122, 1995.

[6] G. Golo and Č. Milosavljević, "Robust discrete-time chattering free sliding mode control," *Systems & Control Letters*, vol. 41, no. 1, pp. 19–28, 2000.

[7] Č. Milosavljević, "General conditions for the existence of a quasi-sliding mode on the switching hyperplane in discrete variable structure systems," *Automation and Remote Control*, vol. 46, no. 3, pp. 307–314, 1985.

[8] Z. Galias and X. Yu, "Complex discretization behaviors of a simple sliding-mode control system," *Circuits and Systems II: Express Briefs, IEEE Transactions on*, vol. 53, no. 8, pp. 652–656, 2006.

[9] ——, "Analysis of zero-order holder discretization of two-dimensional sliding-mode control systems," *Circuits and Systems II: Express Briefs, IEEE Transactions on*, vol. 55, no. 12, pp. 1269–1273, 2008.

[10] B. Wang, X. Yu, and G. Chen, "ZOH discretization effect on single-input sliding mode control systems with matched uncertainties," *Automatica*, vol. 45, no. 1, pp. 118–125, 2009.

[11] V. Acary and B. Brogliato, "Implicit Euler numerical scheme and chattering-free implementation of sliding mode systems," *Systems & Control Letters*, vol. 59, no. 5, pp. 284–293, 2010.

[12] V. Acary, B. Brogliato, and Y. Orlov, "Chattering-free digital sliding-mode control with state observer and disturbance rejection," *Automatic Control, IEEE Transactions on*, vol. 57, no. 5, pp. 1087–1101, 2012.

[13] F. Plestan, V. Bregeault, A. Glumineau, Y. Shtessel, and E. Moulay, "Advances in high order and adaptive sliding mode control–theory and applications," in *Sliding Modes after the First Decade of the 21st Century*, ser. Lecture Notes in Control and Information Sciences. Springer, 2012, vol. 412, pp. 465–492.

[14] M. Defoort, T. Floquet, A. Kokosy, and W. Perruquetti, "A novel higher order sliding mode control scheme," *Systems & Control Letters*, vol. 58, no. 2, pp. 102–108, 2009.

[15] R. Cottle, J.-S. Pang, and R. Stone, *The Linear Complementarity Problem*, ser. Classics in Applied Mathematics. Society for Industrial Mathematics, 2009, no. 60.

[16] C. Edwards and S. Spurgeon, *Sliding Mode Control: Theory and Applications*, ser. Systems and Control Book Series. CRC Press, 1998, vol. 7.

[17] B. Wang, X. Yu, and X. Li, "ZOH discretization effect on higher-order sliding-mode control systems," *Industrial Electronics, IEEE Transactions on*, vol. 55, no. 11, pp. 4055–4064, 2008.

[18] F. Facchinei and J.-S. Pang, *Finite-Dimensional Variational Inequalities and Complementarity Problems*, ser. Springer Series in Operations Research. Springer, 2003.

[19] V. Acary and B. Brogliato, *Numerical Methods for Nonsmooth Dynamical Systems: Applications in Mechanics and Electronics*, ser. Lecture Notes in Applied and Computational Mechanics. Springer Berlin Heidelberg, 2008, vol. 35.

[20] K. Furuta and Y. Pan, "Discrete-time variable structure control," in *Variable Structure Systems: Towards the 21st Century*, ser. Lecture Notes in Control and Information Sciences, J.-X. Yu X., Xu, Ed. Springer Berlin Heidelberg, 2002, vol. 472, pp. 57–81.

[21] C.-F. Lin and W.-C. Su, "A total chattering-free sliding mode control for sampled-data systems," in *American Control Conference, 2004. Proceedings of the 2004*, vol. 3. IEEE, 2004, pp. 1940–1945.

[22] V. Acary and F. Pérignon, "An introduction to Siconos," INRIA, Rapport Technique RT-0340, 2007. [Online]. Available: http://hal.inria.fr/inria-00162911

[23] J. D. Hunter, "Matplotlib: a 2D graphics environment," *Computing in Science & Engineering*, pp. 90–95, 2007.

[24] D. Hinrichsen and A. J. Pritchard, *Mathematical Systems Theory I*, ser. Texts in Applied Mathematics. Springer Berlin Heidelberg, 2005, vol. 48.

[25] V. Utkin, *Sliding Modes in Control and Optimization*, ser. Communications and Control Engineering. Springer Berlin, 1992.

[26] D. Bernstein, *Matrix Mathematics*. Princeton University Press Princeton, NJ, 2005.

[27] R. A. Horn and C. R. Johnson, *Topics in Matrix Analysis*. Cambridge University Press, 1994.

[28] L. Ambrosio, N. Fusco, and D. Pallara, *Functions of Bounded Variation and Free Discontinuity Problems*. Clarendon Press Oxford, 2000.

RESEARCH CENTRE
GRENOBLE – RHÔNE-ALPES

Inovallée
655 avenue de l'Europe Montbonnot
38334 Saint Ismier Cedex

Publisher
Inria
Domaine de Voluceau - Rocquencourt
BP 105 - 78153 Le Chesnay Cedex
inria.fr

ISSN 0249-6399